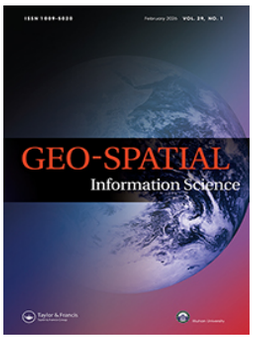

Taylor & Francis
Taylor & Francis Group

Geo-spatial Information Science

ISSN: 1009-5020 (Print) 1993-5153 (Online) Journal homepage: www.tandfonline.com/journals/tgsi20

SARTRAM: SAR-based trapezoid model for water table depth monitoring in restored peatlands

Laurynas Jukna, Elzė Buslavičiūtė, Rasa Janušaitė, Tomas Raila & Leonas Jarašius

To cite this article: Laurynas Jukna, Elzė Buslavičiūtė, Rasa Janušaitė, Tomas Raila & Leonas Jarašius (24 Apr 2026): SARTRAM: SAR-based trapezoid model for water table depth monitoring in restored peatlands, Geo-spatial Information Science, DOI: 10.1080/10095020.2026.2660547

To link to this article: https://doi.org/10.1080/10095020.2026.2660547

GEO-SPATIAL INFORMATION SCIENCE
https://doi.org/10.1080/10095020.2026.2660547

SARTRAM: SAR-based trapezoid model for water table depth monitoring in restored peatlands

Laurynas Jukna[a], Elzė Buslavičiūtė[a], Rasa Janušaitė[a], Tomas Raila[b] and Leonas Jarašius[c]

[a]Institute of Geosciences, Faculty of Chemistry and Geosciences, Vilnius University, Vilnius, Lithuania; [b]Institute of Computer Science, Faculty of Mathematics and Informatics, Vilnius University, Vilnius, Lithuania; [c]Foundation for Peatland Restoration and Conservation, Vilnius, Lithuania

ABSTRACT

Remote sensing has emerged as a valuable tool for monitoring peatland water table depth (WTD), offering local to global-scale observations and high-frequency monitoring capabilities. We present the first attempt to adapt the trapezoidal model concept to SAR, developing the SAR trapezoid model (SARTRAM) for peatland WTD remote sensing. The model is based on the interpretation of the pixel distribution within the surface backscatter-radar vegetation index (RVI) trapezoid space. We used Sentinel-1 and Sentinel-2 data to evaluate and compare the performance of SARTRAM, surface backscatter (γ^o) and the traditional optical trapezoid model (OPTRAM) in 29 restored peatlands and 98 WTD logging sites in Scotland and Lithuania. We employed five different model value extraction methods: value at logger point, average buffer value, best-pixel (BP) within the peatland area, BP within 100 m (BP100m) and 500 m (BP500m) search distance buffers. To enhance performance, a moving average window (MAW) filter was applied to SARTRAM. This study demonstrated that SARTRAM exhibited substantial potential, particularly when temporal MAW filtering was applied, resulting in a 10–19% improvement in correlation with WTD compared to the initial SARTRAM results. SAR backscatter showed an average Spearman correlation coefficient of 0.52 and 0.57 with WTD for BP500m and BP methods (VV polarization), respectively. The model with MAW-filtered SARTRAM achieved average Spearman correlation values of 0.65 and 0.62 with the VH and VV polarization data for the BP and BP500m methods, respectively. OPTRAM outperformed SARTRAM across all value extraction method cases, resulting in average correlation coefficients of 0.85 and 0.83 for the BP and BP500m methods, respectively. Nevertheless, SARTRAM demonstrated slightly better overall results compared to traditional WTD prediction methods based on SAR backscatter signal analysis.

ARTICLE HISTORY
Received 3 November 2024
Accepted 8 April 2026

KEYWORDS
Peatland; groundwater depth; synthetic aperture radar (SAR); trapezoid model; Sentinel-1

1. Introduction

Predominantly situated in high latitudes (~45°–70°) (UNEP 2022; Loisel and Gallego-Sala 2022, Yu et al. 2010), the majority of peatlands store approximately 25% of the global soil carbon stock (Gorham 1991; Köchy, Hiederer, and Freibauer 2015; Leifeld and Menichetti 2018; Yu et al. 2010), equating to half of the carbon content present in the Earth's atmosphere as CO_2 (Drösler et al. 2008). The soil moisture in surface peat layers and the water table depth (WTD) are important features that control the interface between aerobic and anaerobic conditions. This, in turn, may significantly impact the role of peatlands in the carbon cycle, shifting them from a carbon sink to a CO_2 source (Belyea and Malmer 2008; Beyer et al. 2021; Kwon et al. 2022; Loisel et al. 2021; McNeil and Waddington 2003; Nugent et al. 2018; Schwieger et al. 2021). Additionally, peatlands play a crucial role in flood control (Acreman and Holden 2013; Ahmad et al. 2020; Gao, Holden, and Kirkby 2016), maintenance of water quality (Martin-Ortega et al. 2014; Pschenyckyj et al. 2023), and serve as a habitat for many plant and animal species (UNEP 2022; Littlewood et al. 2010).

For centuries, peatlands have been exposed to intense human activities, such as land-use change and drainage, resulting in the degradation of their ecosystems and hydrology (Fluet-Chouinard et al. 2023; Höper et al. 2008; Loisel and Gallego-Sala 2022; Page and Baird 2016). Nowadays, these processes are further accelerated by climate change (Swindles et al. 2019). In recent decades, the restoration of degraded peatlands has been increasingly acknowledged as an important component in climate change mitigation, with most initiatives prioritizing water table (WT) restoration (D'Acunha, Lee, and Johnson 2018; Gatis et al. 2023; Holden et al. 2011; Parry, Holden, and Chapman 2014; Schimelpfenig,

CONTACT Laurynas Jukna laurynas.jukna@gf.vu.lt
Supplemental data for this article can be accessed online at https://doi.org/10.1080/10095020.2026.2660547

Cooper, and Chimner 2014; Shuttleworth et al. 2019). As a crucial parameter to evaluate, peatland WTD is commonly measured using ground-based in-situ techniques (Kartiwa et al. 2023; Nijp et al. 2019; Whittington et al. 2007). Despite providing accurate results, in-situ measurements are relatively expensive and oriented toward single, small-area observations, making them less effective for mapping spatial variations in large peatland areas. Additionally, due to their relative inaccessibility, peatlands are also considered challenging areas to monitor. All of this serves as a strong motive to deploy satellite remote sensing, allowing for the continuous and cost-effective spatio-temporal monitoring of water table dynamics in large spatial extents.

In recent years, remotely sensed WTD studies have predominantly focused on using three distinct types of satellite sensors: active microwave (synthetic aperture radar (SAR)), passive microwave (passive radiometers), and passive optical (visible, near-infrared (NIR), shortwave infrared (SWIR), and in some cases thermal range operating multispectral optical sensors) (Räsänen, Tolvanen, and Kareksela 2022). Two predominant techniques for determining WTD can be identified in studies employing active microwave radar satellite sensors. The primary and most frequently applied technique involves the application of incoherent backscatter strength analysis (Asmuß, Bechtold, and Tiemeyer 2018, 2019; Dabrowska-Zielinska et al. 2016; Isoaho et al. 2024; Jaenicke, Englhart, and Siegert 2011; Kasischke and Bourgeau-Chavez 1997; Kasischke et al. 2008; Kim et al. 2017; Krzepek, Schmidt, and Iwaszczuk 2022; Lees et al. 2021; Mohammadimanesh et al. 2018a, 2018b; Räsänen, Tolvanen, and Kareksela 2022; Reddin et al. 2025; Toca et al. 2023; Torbick et al. 2012). The secondary, less commonly used approach is associated with the analysis of bulk peat movement through the coherent differential phase component of the signal (Chen et al. 2020; Hrysiewicz et al. 2023; Kim 2013; Mohammadimanesh et al. 2018a; Tampuu et al. 2020; Walker et al. 2025). In both instances, predominantly C-band sensor data are employed (Sentinel-1, Radarsat-2, ENVISAT-ASAR, ERS-1, ERS-2), while less frequently, L-band (ALOS PALSAR-1) and X-band (TerraSAR-X) sensors have been used. The advantages of SAR data application are primarily associated with its relatively high spatial resolution and insensitivity to weather conditions. Additionally, it exhibits a strong signal sensitivity to soil moisture content (Asmuß, Bechtold, and Tiemeyer 2018; Toca et al. 2022). However, despite these advantages, most studies utilizing microwave backscatter signals over natural peatlands demonstrate ambiguous results (Räsänen, Tolvanen, and Kareksela 2022). Some report relatively low (Krzepek, Schmidt, and Iwaszczuk 2022), whilst others moderate (Asmuß, Bechtold, and Tiemeyer 2018, 2019; Bechtold et al. 2018; Millard et al. 2018) or even high-performance (Klinke et al. 2018; Lees et al. 2021) rates. Passive microwave electromagnetic spectrum sensors, such as SMOS or SMAP, show strong correlations with WTD (Bechtold et al. 2020). However, SMOS and other passive microwave sensors (SMAP, ASCAT) have clear drawbacks, particularly due to their low spatial resolution, which significantly limits their suitability for small-scale area research. The primary focus of optical multispectral satellite instrument applications has been on the use of various spectral indices (D'Acunha, Lee, and Johnson 2018; Harris and Bryant 2009; Isoaho et al. 2024; Linkevičienė et al. 2023; Meingast et al. 2014; Räsänen, Tolvanen, and Kareksela 2022; Reddin et al. 2025; Šimanauskienė et al. 2019). These indices can be classified into groups of water-sensitive and chlorophyll-sensitive indices. Water-sensitive indices are primarily derived from SWIR and NIR bands, with some indices utilizing combinations of visible bands, such as green and red. Chlorophyll-sensitive indices generally involve data from NIR and visible spectrum bands, specifically green or red. It is generally accepted that the accuracy of WTD prediction based on optical spectral indices, in most instances, surpasses SAR-based analysis (Räsänen, Tolvanen, and Kareksela 2022). Also, the latest generation multispectral satellite sensors maintain high spatial resolution, which is preferred in small-scale peatland area research. Nevertheless, the sensitivity to atmospheric conditions (i.e. cloud cover) is a major limitation of optical satellite data (Reynolds, Mota, and Nightingale 2025), which makes it difficult to perform time-consistent observations with high temporal frequency.

In recent years, a novel method based on optical multispectral satellite data has gained widespread acceptance. Introduced by Sadeghi et al. (2017) and subsequently employed by Burdun, Bechtold, Sagris, Komisarenko, et al. (2020), Burdun, Bechtold, Sagris, Lohila, et al. (2020), Burdun et al. (2023), the optical trapezoid model (OPTRAM) demonstrates high correlations with peatland water table fluctuations. Although OPTRAM was originally designed for optical data, SAR signal sensitivity to soil moisture and applicability in vegetation cover monitoring through radar vegetation index (RVI) (Nasirzadehdizaji et al. 2019) adaptation enables the application of trapezoid model principles to SAR data. Implementation of the SAR-based trapezoid model could potentially enhance the frequency of consecutive observations for the satellite-based WTD fluctuation analysis.

As far as we are aware, there have been no published attempts to do this. To fill this gap, we aimed to modify and thus adapt the trapezoid model concept to SAR data, here referred to as SARTRAM, using satellite and WTD data from 29 peatlands in Scotland and Lithuania. The specific objectives of this study were: (i) to adapt the trapezoid model

concept to SAR Sentinel-1 C-band data, (ii) to evaluate the performance of the SAR-based trapezoid model (SARTRAM) in predicting restored peatland WTD, and (iii) to compare the capabilities of SARTRAM with traditional OPTRAM and SAR backscatter γ^o data in restored peatland WTD monitoring.

2. Materials and methods

2.1. Study area

Within the scope of this study, 4 peatland sites in Lithuania and 25 in Scotland were investigated. The chosen sites are located between 54°N and 57°N latitude (Figure 1). The peat thickness in all investigated

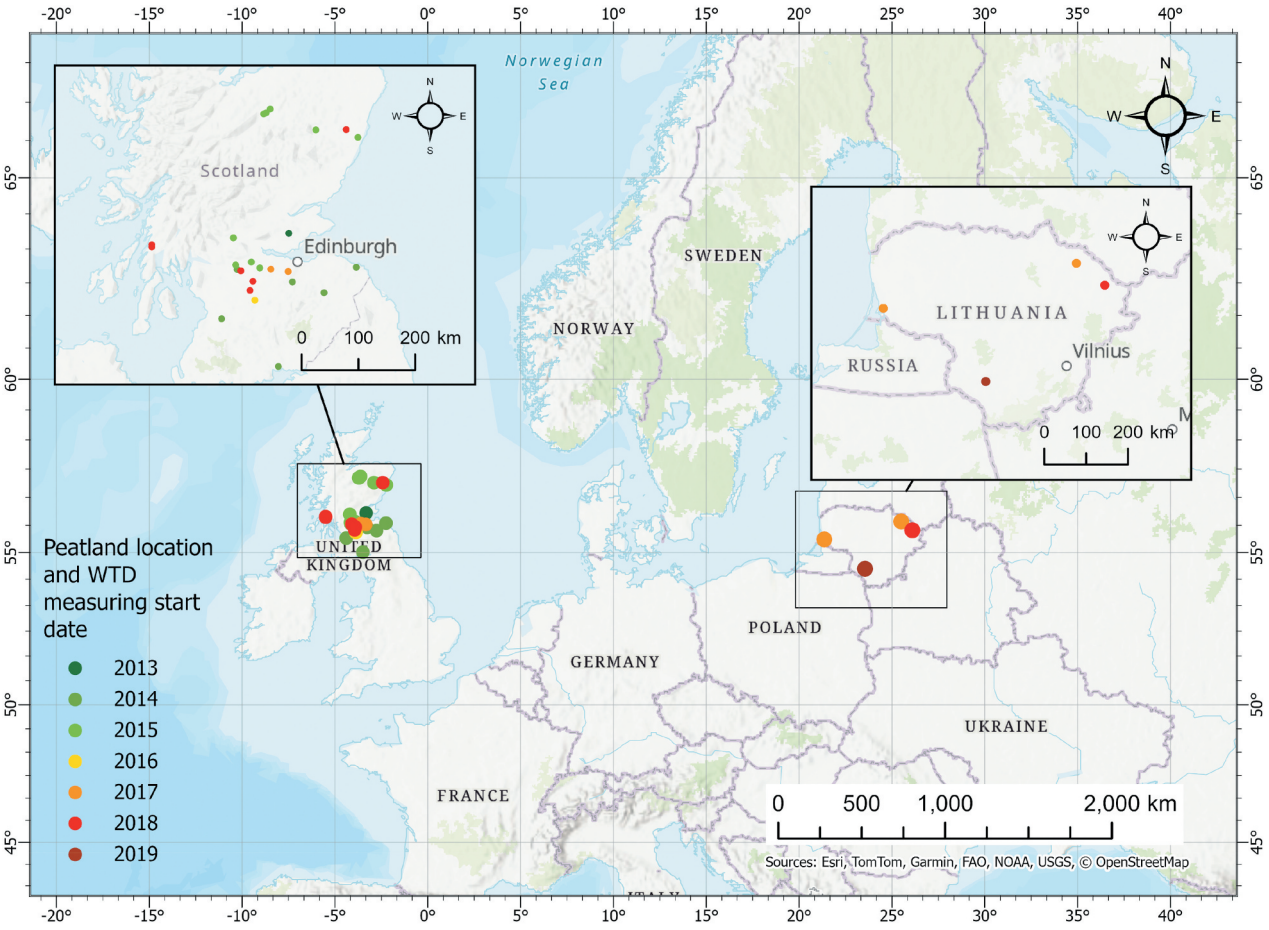

Figure 1. Locations of the 29 peatland study areas. Four areas are located in Lithuania, and 25 are located in Scotland.

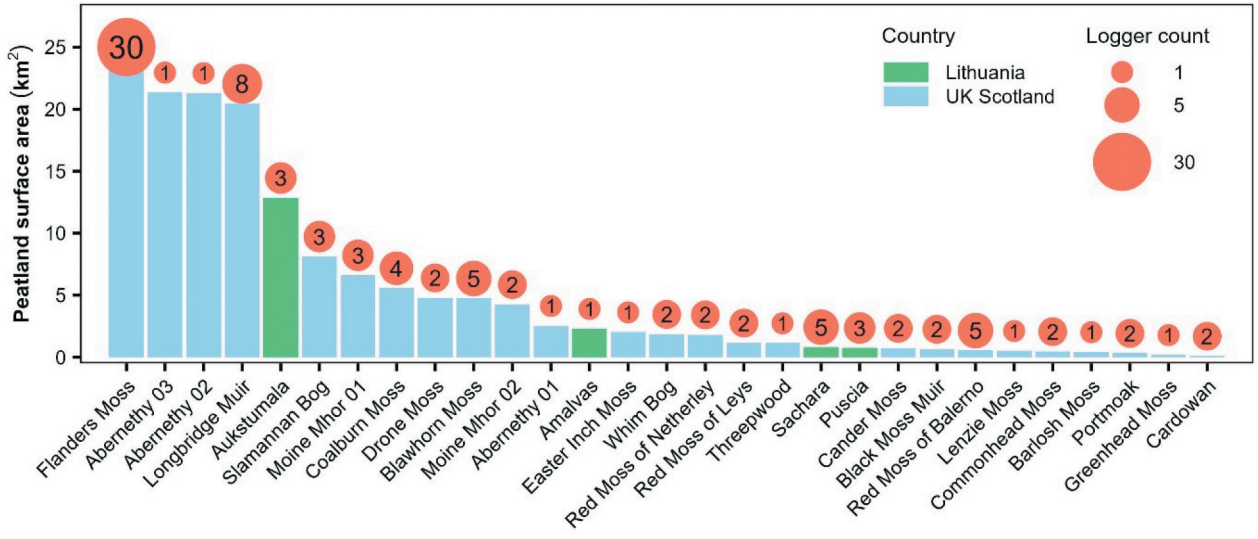

Figure 2. Surface area of studied peatlands and logger count in each peatland.

sites exceeds 30 cm. All peatlands fall under the classification of raised bogs.

The surface area of the peatlands varies from very small (0.08 km^2) to large (23.41 km^2) (Figure 2). All the peatlands included in this study have historically been affected by drainage and cultivated for agriculture (by grazing or plowing), forestry (by drainage to improve tree volume), or peat extraction activities. Over the last decade, peatland restoration programs have been initiated for all the sites. Under the Scotland Nature Agency Peatland Action program, restoration measures started in 2013 (Peatland Action 2024). In Lithuania, restoration was initiated by various NGOs (Foundation for Peatland Restoration and Conservation, Lithuanian Fund for Nature, Nature Heritage Fund) and the State Service for Protected Areas, taking place between 2017 and 2020. The main restoration measures undertaken included tree removal and ditch blocking to raise WT levels (Pakalne et al. 2021). Restoration descriptions and start dates for each site are available in Appendix 1.

2.2. Data

2.2.1. In-situ water table data

To measure WT levels in both locations – Scotland and Lithuania, automatic loggers were employed. In total, data from 98 loggers (86 for Scotland and 12 for Lithuania) were used. The available data spans different time periods for each location. In Lithuania, the WT data generally covers the years from 2017 to 2021, while in Scotland, the data extends over a longer period, from 2013 to 2022. WT data from the Scotland Nature Agency Peatland Action program is publicly available through the program's website (Peatland Action 2024) and is free to use for research purposes. The WT data for Lithuanian peatlands was provided by the Foundation for Peatland Restoration and Conservation. All locations in Scotland were measured at daily and monthly temporal resolutions, while locations in Lithuanian peatlands were measured at 3-h intervals. To align the Lithuanian peatland data with the Scottish dataset and with remote sensing data from Sentinel-1 and Sentinel-2 satellites, it was averaged to daily WT means. Logger name abbreviations used in this article and their respective original names are provided in Appendix 1.

2.2.2. Satellite remote sensing data

Publicly available SAR and optical multispectral data from European Space Agency Copernicus missions Sentinel-1 and Sentinel-2 were used. Satellite data covered the period between 2015 and 2022, depending on WT data availability from individual peatlands and loggers. On average, for all 98 WT logging sites, 326 Sentinel-1 SAR observation dates were used. For Sentinel-2, the average number of observations was much lower, with 34 dates per logger. The highest number of observations for Sentinel-1 was recorded for one logger from the Barlosh Moss site with 420 observations, and 25 loggers from the Flanders Moss site with 419–420 observations. For Sentinel-2, sites with the highest observation number were Black Moss (BLACK1 and BLACK2 loggers) with 84 observations, and Sachara (S1-5 loggers), Puščia (P3-5), and Aukštumala (A8-10) sites with >60 observation dates (Figure 3).

For both Sentinel-1 and Sentinel-2, data were obtained for the growing season (April–October), as other months might have been affected by snow coverage and frost. Dates when the water level was higher than the peatland surface (i.e. inundation dates) were excluded to prevent having specular reflection in the images.

C-band SAR Sentinel-1 GRD data (RVI, VV linear, and VH linear) with a 10-m resolution and a 6-d revisit time were used to calculate SARTRAM. The data were obtained from Google Earth Engine (Gorelick et al. 2017). All acquisitions were acquired in an ascending orbit, minimizing the dew effect during the ascending overpass time of 6 pm (Toca et al. 2023). Additionally, the original SAR backscatter signal (γ^o), expressed in both linear units and decibels (dB), was utilized to evaluate its performance in predicting WTD, in comparison to SARTRAM.

Optical Sentinel-2 data, with 13 spectral bands, spatial resolutions ranging from 10 to 60 m, and a 5-d revisit time (at the equator), was downloaded from the dataset available on Google Cloud Storage. Atmospherically corrected Sentinel-2 Level 2A products were used for the analysis. Sentinel-2 Level 2A Surface Reflectance products are available for dates from 2017. Therefore, for dates in 2015–2017, Sentinel-2 Level 1C products were downloaded and atmospherically corrected to match Level 2A products using the Sen2Cor algorithm (Main-Knorn et al. 2017). Images were filtered based on cloud percentage. It was set to up to 30% when filtering Sentinel-2 tiles for download, but during data preprocessing, only the images with a cloud cover below 10% over the studied peatland extent were selected. All Sentinel-2 data downloading and preprocessing steps were implemented via R using the "sen2r" package (Ranghetti et al. 2020).

2.2.3. Data processing steps

For Sentinel-1 data, the preprocessing algorithm developed by Mullissa et al. (2021) was employed to address border noise, conduct multi-temporal Lee Sigma filtering (with a kernel size and image collection set to 5), and perform radiometric terrain normalization using STRM's 30-m resolution DEM, resulting in γ^o backscatter. We adhered to this coarser resolution

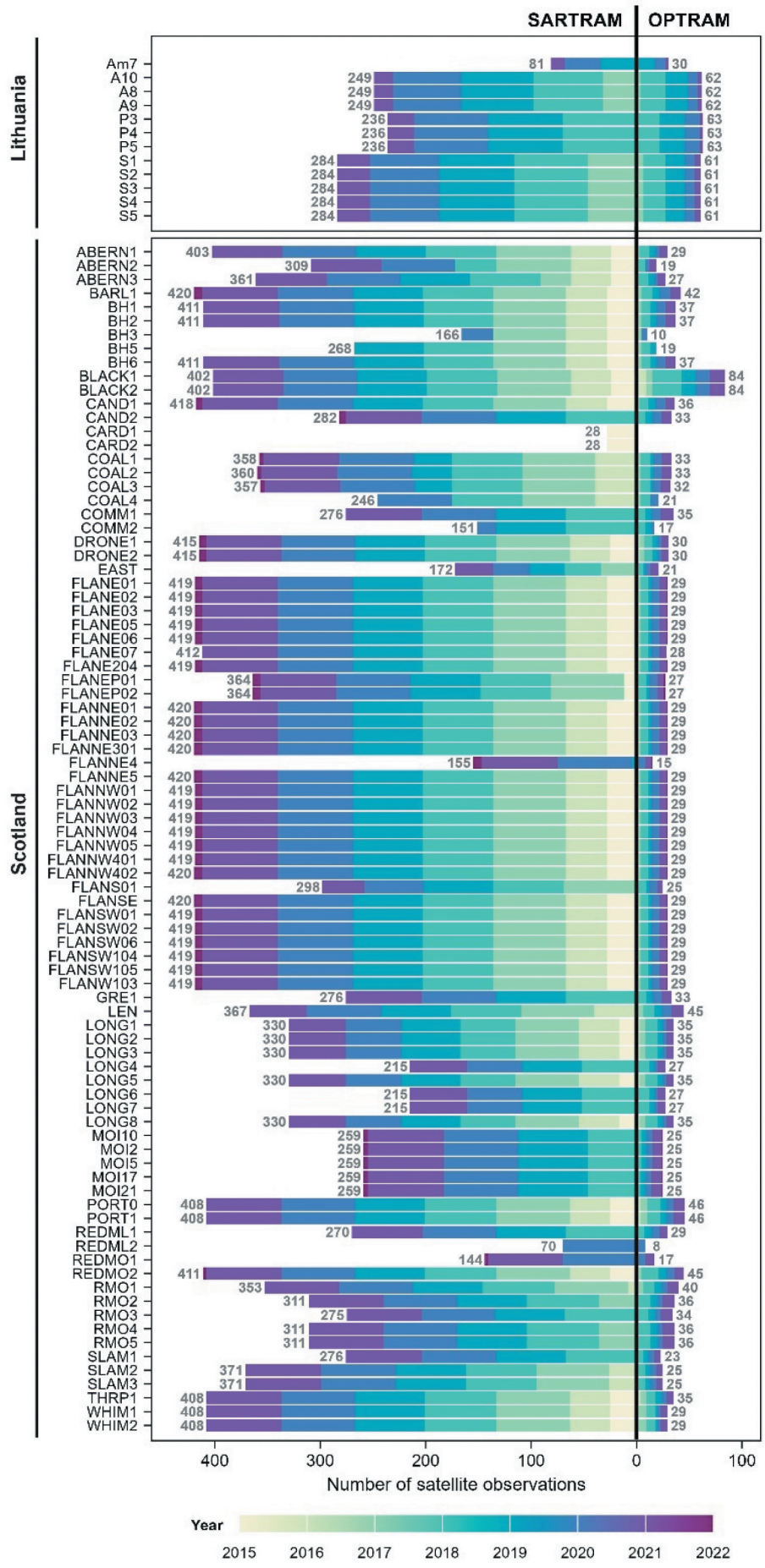

Figure 3. Count of Sentinel-1 and Sentinel-2 satellite data observations used in the study for each peatland WT logging site.

DEM due to the unavailability of higher-resolution DEMs in the majority of Scotland.

As the quality of optical satellite data frequently suffers from the presence of cloud cover, clouds and cloud shadows in Sentinel-2 images were masked based on Sen2Cor scene classification (SCL), including classes of medium- and high-probability clouds, thin cirrus, cloud shadows, and no data. Sentinel-2 bands with resolutions of 20 and 60 m were resampled to a resolution of 10 m using the nearest neighbor method. Images were clipped by the peatland areas and merged into multiband rasters.

2.2.4. OPTRAM calculation

To obtain multitemporal OPTRAM values from Sentinel-2 satellite data for the investigated peatland sites, we followed Sadeghi et al. (2017) methodology, where a trapezoid is formed by normalized difference vegetation index (NDVI) as a measure of vegetation cover and shortwave infrared transformed reflectance (STR) as a measure of moisture content. For the delineation of primary dry and wet edges, initially, the R code provided by Burdun, Bechtold, and Komisarenko (2022) was adapted and employed. Nevertheless, the presence of pixel oversaturation frequently led to inaccuracies in the determination of the wet edge, necessitating further manual adjustments based on visual inspection.

2.2.5. SARTRAM calculation

By adapting the trapezoid model concept to SAR data and proposing it as the SAR trapezoid model, we hypothesize that, similar to OPTRAM, SARTRAM can help determine the temporal changes in WTD.

Unlike traditional SAR backscatter signal-based WTD observation techniques, SARTRAM utilizes two signals: vegetation chlorophyll information from the RVI and moisture information from SAR backscatter signal γ^o. Consequently, SARTRAM relies on two assumptions: (i) a linear relationship between soil moisture and γ^o, and (ii) a linear relationship between soil (in this case, peat) and vegetation moisture content.

(i) First, SAR backscatter signal sensitivity to soil moisture is explained by the difference between the dielectric constants of water (~80) and soil particles (~4) (Mohan et al. 2015; Schmugge et al. 1974). Second, a direct linear relationship between surface soil moisture and SAR intensity (in dB) was demonstrated by Ulaby, Moore, and Fung (1986). Later, this relationship was applied in various soil moisture-related studies (Esch 2018; Le Hégarat-Mascle et al. 2002; Quesney et al. 2000; Zribi et al. 2005). Third, Toca et al. (2022) recently demonstrated a strong sensitivity of backscattering strength to hydrological patterns in a peatland ecosystem, indicating that moisture is the primary factor controlling backscattering values. This finding also aligns with the results of Asmuß, Bechtold, and Tiemeyer (2019), who identified WTD as the primary determinant of backscattering strength in drained temperate grasslands with underlying peat soils.

(ii) *Sphagnum* mosses are the dominant vegetation in most peatlands in temperate and high-latitude regions. *Sphagnum* mosses lack roots and internal water-conducting tissue (Tuba, Slack, and Stark 2011). They absorb water directly through their surface (Hyyryläinen et al. 2018). Consequently, the water content in *Sphagnum* responds strongly to fluctuations in peat moisture and WTD. Water retained within *Sphagnum* is primarily influenced by water availability from precipitation, peat moisture, and most importantly – WT (Gong et al. 2020; Harris, Bryant, and Baird 2006).

To conclude, if both assumptions are met, SARTRAM values can further be calculated in a projected two-dimensional γ^o- RVI space.

Usually, when utilizing OPTRAM, the moisture-sensitive signal (STR) is combined with a vegetation index (VI) to construct a trapezoid space. The highest STR values along the vegetation cover gradient define the areas with the highest soil moisture content, whereas the lowest STR values define the areas with the lowest soil moisture content. This trapezoid space is then used to linearly scale soil moisture (Babaeian, Bechtold, Sagris, Komisarenko, et al. 2020; Burdun, Bechtold, Sagris, Lohila, 2020; Burdun et al. 2023; Sadeghi et al. 2017). To construct a trapezoid space for SARTRAM, we combined RVI as the target vegetation index and Sentinel-1 backscatter signal (γ^o) in VH and VV polarization as an indicator of soil moisture (Figure 4). The validity of the vegetation index used in trapezoidal models is conditional on its sensitivity to chlorophyll content (and hence, to soil water content). As referred to in Burdun et al. (2023), the choice of vegetation index does not significantly affect trapezoid model performance. Hence, in the case of optical data-based trapezoid models, the most common vegetation index used is NDVI. In the SARTRAM case, we assume RVI meets the necessary conditions. Originally created by Kim and Van Zyl (2009), modified for dual-polarization SAR data by Trudel, Charbonneau, and Leconte (2012), and adapted for Sentinel-1 data by Nasirzadehdizaji et al. (2019), RVI is known as an index suitable for vegetation monitoring (Holtgrave et al. 2020; Kumar, Rao, and Sharma 2013). Some studies suggest that RVI is less sensitive to environmental condition changes

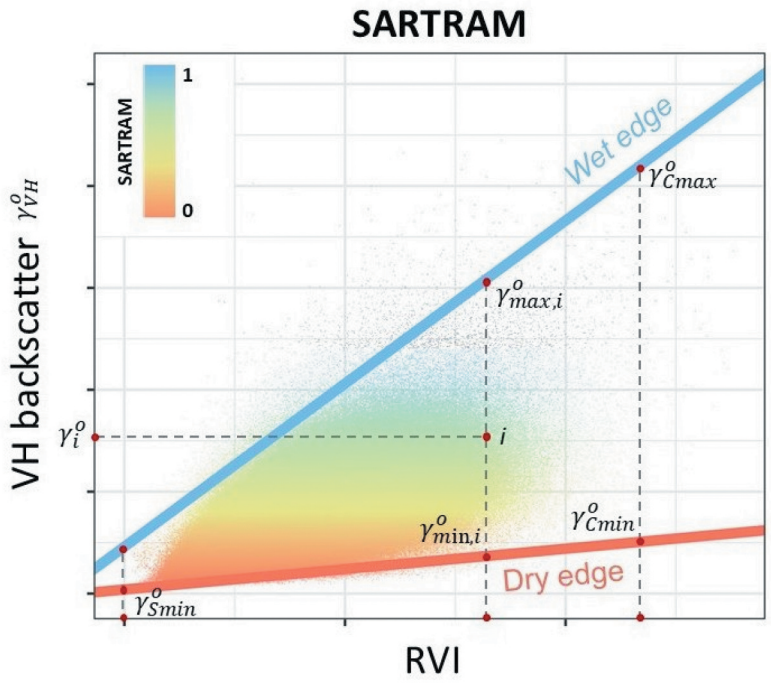

Figure 4. Illustration of the concept of the SAR trapezoid model. The image is based on the Amalvas peatland dataset. VH backscatter is the vertical-horizontal polarization backscatter signal (in linear units); RVI is the radar vegetation index; γ^o_i is the γ^o value of pixel *i*; $\gamma^o_{max,i}$ and $\gamma^o_{min,i}$ are γ^o values of the dry and wet edge at the RVI of the pixel *i*, respectively.

(such as soil moisture) than single-polarization backscatter and is suitable for monitoring vegetation phenological patterns, as well as biomass and vegetation moisture content (Kim and Van Zyl 2009; Kumar, Rao, and Sharma 2013).

To calculate RVI from Sentinel-1 data, we followed the methodology outlined by Holtgrave et al. (2020), where γ^o_{VH} represents the backscatter in single VH polarization and γ^o_{VV} represents the backscatter in single VV polarization.

$$RVI = \frac{4 \times \gamma^o_{VH}}{\gamma^o_{VH} + \gamma^o_{VV}} \quad (1)$$

As a measure of soil moisture, we used Sentinel-1 original signal backscatter values γ^o(we tested both γ^o_{VV} and γ^o_{VH} polarisations).

$$W_{SARTRAM_{\gamma^o},i} = \frac{\gamma^o_i - \gamma^o_{min,i}}{\gamma^o_{max,i} - \gamma^o_{min,i}} \quad (2)$$

where γ^o_i is the γ^o value of pixel *i*, $\gamma^o_{max,i}$ and $\gamma^o_{min,i}$ are γ^o values of the dry and wet edge at the RVI of the pixel *i*, respectively.

To calculate the wet and dry edge for SARTRAM, we used the same approach as in the case of OPTRAM, which has been used in numerous studies (Babaeian et al. 2018; Burdun et al. 2023; Sadeghi et al. 2017).

$$\gamma^o_{min,i} = int_{min} + s_{min} \times RVI \quad (3)$$

$$\gamma^o_{max,i} = int_{max} + s_{max} \times RVI \quad (4)$$

where int_{min} and S_{min} are the intercept and slope of the dry edge, respectively, and int_{max} and S_{max} are the intercept and slope of the wet edge, respectively. The wet edge is formed by the pixels with the highest γ^o values along the RVI gradient. These pixels are assumed to have the wettest conditions. The dry edge is formed by the pixels with the lowest γ^o values along the RVI gradient with the presumably lowest moisture availability (and deepest WTD). γ^o–RVI trapezoid space is constructed using a time series of all pixels within the studied site. As in OPTRAM's case, we parameterized SARTRAM's final wet and dry edges by visual inspection.

It is important to mention that within the γ^o–RVI space, SARTRAM values for pixels sharing the same γ^o values will differ if their positions along the RVI gradient axis vary. This indicates a scenario in which the γ^o value for particular pixels could be recorded at different stages of the vegetational season or within different types of peatland vegetation cover. Similarly, identical RVI values, but differing γ^o values will also signify distinct SARTRAM pixels. In the latter case, peatland areas representing the same vegetation type would exhibit variations in γ^o scattering due to WTD-induced scattering differences. Specifically, a deeper WTD would result in a weakened γ^o signal, whereas a shallower WTD would lead to signal amplification. In this way, similar to other trapezoidal models, SARTRAM accounts for the vegetation type-specific relationships, which is also pertinent to SAR vegetation phenology and classification studies (Del Frate et al. 2003; Skriver 2012; Udali, Lingua, and Persson 2021; Xu et al. 2019).

Due to specular reflectance, γ^o–surface soil moisture relationship is valid for partially and fully saturated soil, but not for inundation conditions. For this reason, pixels incorporating standing water should be eliminated from the analysis process.

2.2.6. Data analysis

Other WTD remote sensing studies in peatlands show high variations in correlation or regression analysis results (Abdelmajeed and Juszczak 2024; Asmuß, Bechtold, and Tiemeyer 2018, 2019; Burdun, Bechtold, Sagris, Komisarenko, et al. 2020; Burdun, Bechtold, Sagris, Lohila, et al. 2020; Burdun et al. 2023; Kim 2013; Lees et al. 2021; Millard et al. 2018; Räsänen, Tolvanen, and Kareksela 2022; Šimanauskienė et al. 2019). This is usually explained by differences between study sites (natural or drained, restored or not), the locations of WT loggers, the density of wooded vegetation in the area, and WTD depth (Millard and Richardson 2018; Räsänen, Tolvanen, and Kareksela 2022). As a result of these factors, the satellite image pixel most sensitive to WTD may not necessarily coincide with the location of the logger. To address this issue, Burdun, Bechtold, Sagris, Lohila, et al. (2020) introduced the best pixel technique, where the pixel that has the highest correlation with WTD within the peatland area is considered as best-pixel and used for the WTD prediction. In this study, in addition to pixel values corresponding to the WT logger location point (PTS), an average 25-m buffer around the logger point values (BUFF25m) was extracted for SARTRAM, surface backscatter γ^o and OPTRAM, alongside the best pixel for the entire peatland area (BP). We also supplemented the original best-pixel approach, calculating the best-pixel values for 100-m (BP100m) and 500-m (BP500m) buffers around the logger point.

Linear regression was employed to estimate the relationship between a SARTRAM, OPTRAM, and SAR backscatter signal (γ^o) variable as the predictor and WTD as the target variable. The accuracy of the linear models was assessed by calculating Spearman correlation coefficients (R) and the root mean squared error (RMSE) of the predicted and actual WTD values. These models were used to compare the performance of OPTRAM and SARTRAM, as well as SARTRAM and SAR backscatter signal (γ^o) (calculated in both linear units and decibels (dB)) in monitoring WTD fluctuations. Spearman's correlation was selected over alternative methods due to the non-normal distribution of WTD data in most (95%) loggers, which was tested with the Anderson-Darling Normality Test (p-value of 0.05).

To demonstrate that the observed relationships are not driven by temporal autocorrelation, an anomaly correlation was additionally performed. Anomalies for both the WTD and SARTRAM time series were calculated by computing monthly means across the years and subtracting them from the original WTD and SARTRAM values. The resulting WTD and SARTRAM anomalies were then correlated, enabling a comparison between the original and anomaly-based correlations.

For further analysis steps, a time series of SARTRAM data for each site and logger was smoothed by calculating the moving average (MAW) with a window size of 3 data points. WTD prediction capabilities of temporally filtered and unfiltered SARTRAM were then compared using linear regression. To evaluate SARTRAM performance at the vertical WTD scale, a segmented regression analysis with one breaking point was used. The existence of a single breakpoint was tested with the Davies test (p-value of 0.05), while the linear model fit in both segments was expressed by R and RMSE values.

3. Results

3.1. WTD variations between study sites

Water table depth data showed that Lithuanian sites exhibited deeper WTD values and higher temporal WTD fluctuations than Scottish peatland sites, with multiannual average WTD values of −24.24 and −10.84 cm and multiannual average standard deviations of 16.61 and 8.10 cm for Lithuanian and Scottish peatlands, respectively (Figure 5). Most of the sites had multiannual average WTD values between −5 and −18 cm, with the exception of Amalvas, Sachara, Moine Mhor 01, and Cardowan that had deeper WTD conditions (−35.64–-22.77 cm) and Red Moss of Netherlay as well as Abernethy 03 with nearly inundation conditions (Figure 5). Sites with the deepest average WT levels also demonstrated the highest multiannual variability in WTD values (Figure 5).

Lithuanian and Scottish peatlands exhibited different seasonal WTD fluctuations, with the water level being the highest in autumn (September–October) for Scotland (−11.59 cm, on average) and in spring (April–May) for Lithuania (−19.36 cm, on average), and the lowest in summer (June–August) (−16.19 cm, on average) and summer–autumn (−34.63–-33.4 cm, on average) for Scotland and Lithuania, respectively (Figure 5).

3.2. Correlation of SARTAM and OPTRAM with WTD

Figure 6 shows WTD correlation with SARTRAM VH, SARTRAM VV, and OPTRAM variables for different spatial trapezoid model value extraction models: BP100m, BP500m, and BP, as well as BUFF25m and PTS at WTD logger location.

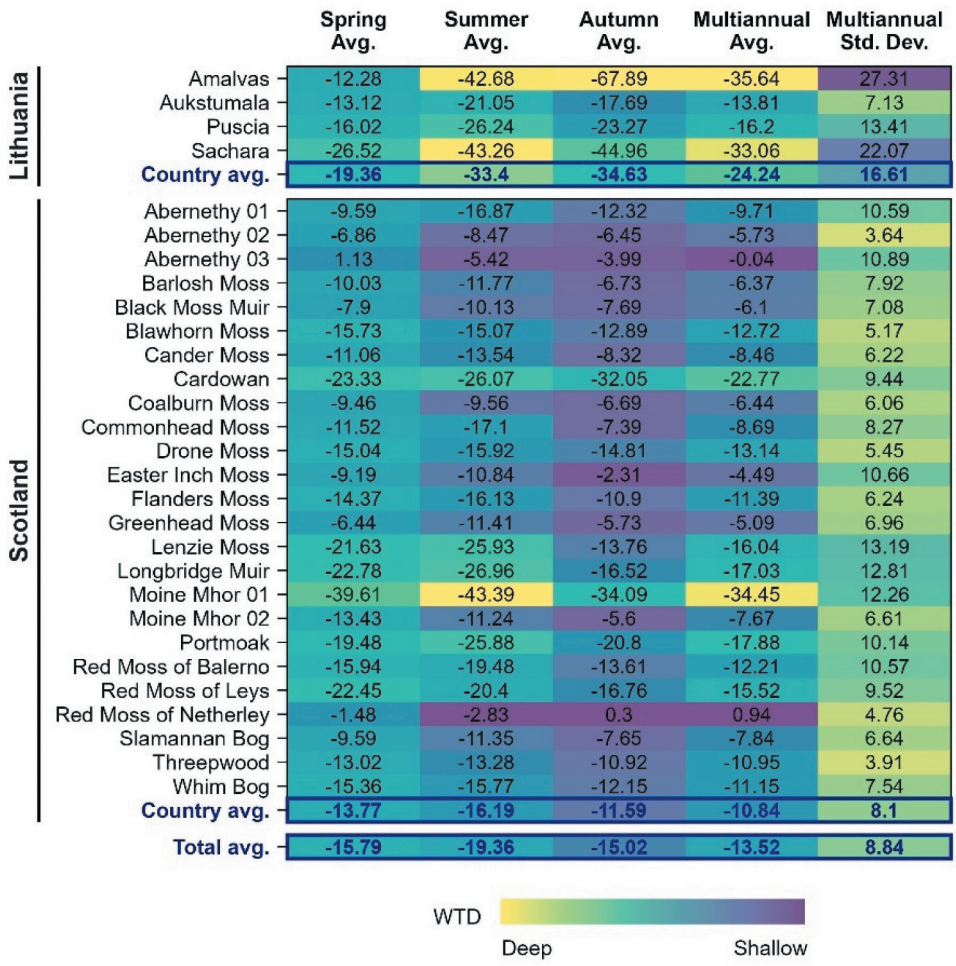

Figure 5. Water table depth statistics at seasonal and multiannual scales for the study peatlands (Avg.: Average; Std. Dev.: Standard deviation values).

A few general patterns emerge from the obtained results. First, both OPTRAM and SARTRAM predominantly demonstrate positive correlations with WT dynamics. Second, OPTRAM outperforms SARTRAM, obtained with both VH and VV polarizations for all model value extraction cases. The best results for both OPTRAM and SARTRAM were observed with the BP model, where average *R* and RMSE values were 0.85 and 4.63 cm, 0.59 and 7.48 cm, and 0.58 and 7.52 cm for OPTRAM, SARTRAM VH, and VV, respectively. The poorest WTD prediction results were observed for the PTS and the BUFF25m models, with the latter showing slightly better performance compared to the former. For these models, the correlation values obtained for SARTRAM VH and VV were low, and the RMSE values were high.

OPTRAM PTS and BUFF25m models showed a relatively higher performance, but still the lowest among all OPTRAM value extraction methods (Figure 7). Third, comparing the correlations between different best pixel value extraction models shows that the *R*-value increases as the diameter of the best pixel search buffer increases.

For the BP500m model, the WTD correlations with both OPTRAM and SARTRAM were higher for all research sites than those for the 100-m buffer (BP100m) and slightly inferior to the correlations for the BP model. Within some specific study sites, the *R* values remained the same or very close for both the BP500m and BP models (Figure 6). Fourth, SARTRAM calculated with VH polarization on average performed similarly to VV polarization, with the exception of a slight increase in *R* values in the BP and PTS VH polarization models.

Because of limitations in spatial resolution and the possible small-scale variations in observation area physical conditions (topography and microtopography, variation in vegetation cover, short-term inundations, overall WTD), SAR data-based products can demonstrate not only high spatial but also temporal variations. Figure 8 shows the correlation between SARTRAM VH and SARTRAM VV values, obtained through different value extraction methods, with applied temporal data filtering, and WTD at the analyzed study sites (Figure 8). As indicated by higher *R* coefficients and lower RMSE, the applied moving average window (MAW) improved the linear relationship between the measured features and the variable (Figure 9).

The average *R* values obtained with BP were 0.65 for SARTRAM VH and VV, while the RMSE

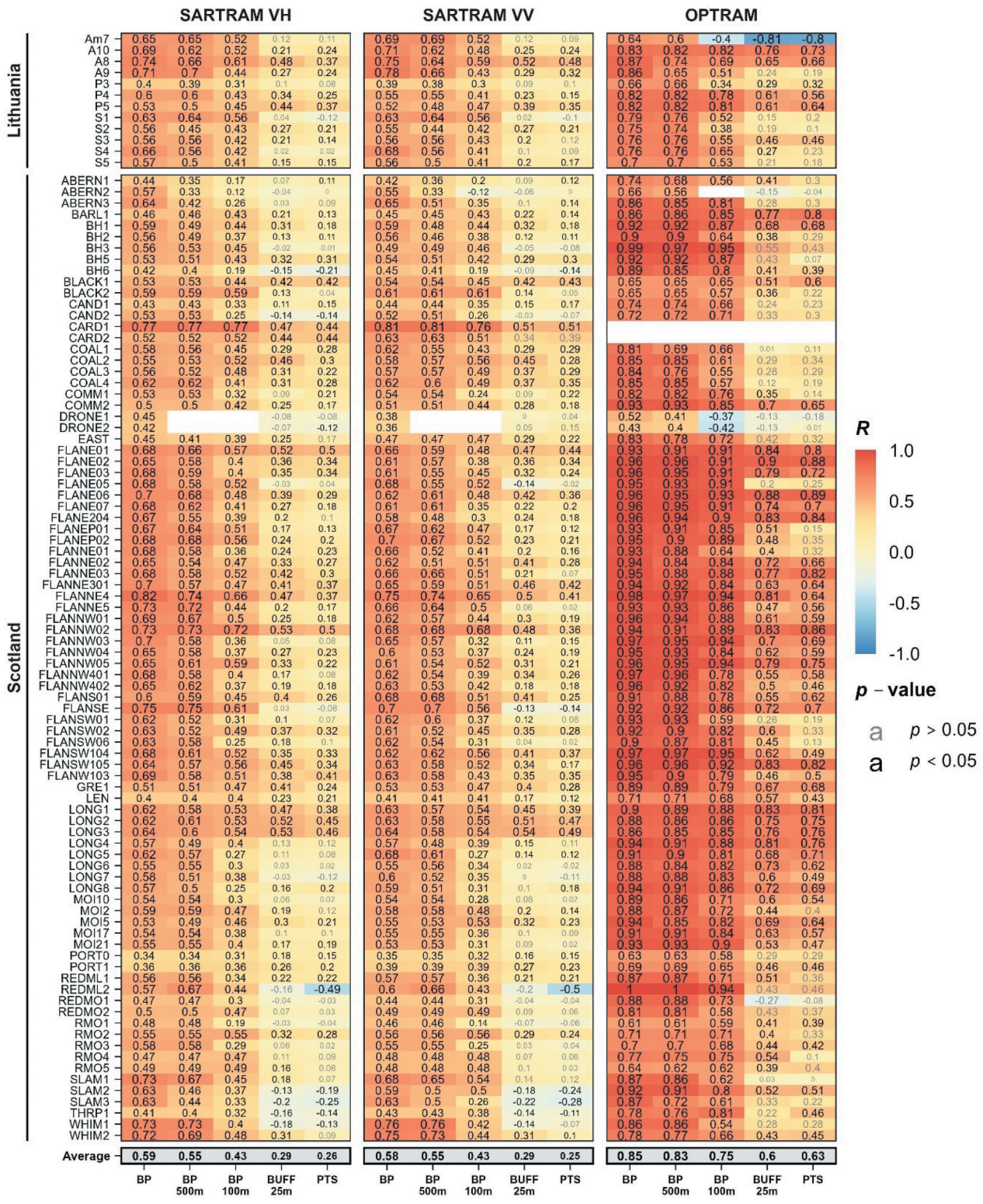

Figure 6. Spearman correlation between WTD and SARTRAM VH and VV polarization and OPTRAM (S2) data calculated for PTS, BUFF25m, BP100m, BP500m, and BP models. Correlation values are given for all 98 logger sites in 29 peatlands.

values were 6.89 cm and 6.91 cm for VH and VV polarizations, respectively. The BP500m model correlations with WTD were slightly lower and reached 0.62 for VH and VV polarization, while RMSE reached 7.13 and 7.19 cm for VH and VV polarizations. BP100m model correlations with WTD for both VH and VV polarizations were 0.51, and RMSE was 7.69 cm (Figure 9).

Despite the increase in SARTRAM performance, as with the unfiltered data, PTS and BUFF25m models demonstrated the lowest correlation with WTD values. The trend of the best-pixel correlation decrease and RMSE increase with the decrease in buffer diameter remained consistent.

From the perspective of temporal data, WTD time series are often autocorrelated, which

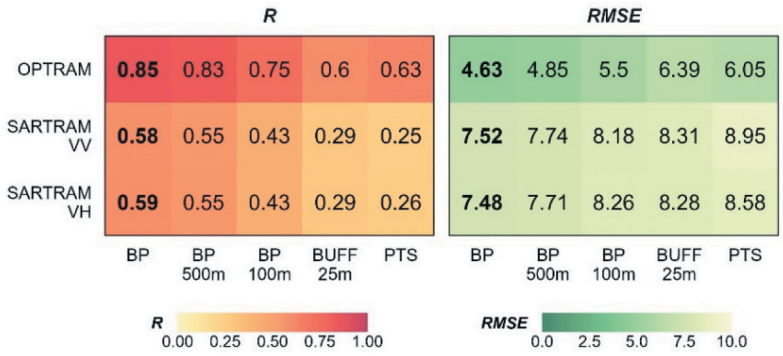

Figure 7. The average *R* and RMSE values for all SARTRAM- and OPTRAM-based WTD prediction models.

complicates correlation calculations as it violates the assumption of independent data points. In this case, the calculated average Spearman anomaly correlations closely matched the original Spearman correlations in value (Appendix 3), suggesting that the observed relationship may exist independently of autocorrelation effects. Additionally, Appendix 4 presents the time series comparison of WTD and SARTRAM with MAW for the best-performing BP and BP500m models, showing similarity in trends across most loggers.

To account for the substantial difference in observation counts between Sentinel-1 and Sentinel-2 satellite data (Figure 3), the SARTRAM time series was additionally aligned with Sentinel-2 using a fuzzy join within a ± 2-d window, when exact date matches were unavailable. This ensured a comparable number of observations across both methods, resulting in 3023 matched observations across all loggers. The average *R* for OPTRAM ranged from 0.62 to 0.82, outperforming SARTRAM, which exhibited lower *R* values of 0.48–0.60 for VV and 0.46–0.60 for VH (without MAW) across all value extraction cases. This suggests that OPTRAM remains superior even when SARTRAM is limited to a shorter time series. The highest average *R* values were consistently achieved using the BP model, while the lowest were observed with the PTS model, except in the case of the OPTRAM BUFF25m model, which performed worse than the PTS model. Regarding RMSE for linear regression models, SARTRAM ranged from 6.48 to 7.45 for VV and 6.51 to 7.54 for VH, whereas OPTRAM demonstrated lower RMSE values, ranging from 4.34 to 6.53. Notably, the average statistically significant *R* values for the shorter SARTRAM time series (Appendix 6) were not lower than those for the longer SARTRAM series (Figure 7), indicating that the initially observed correlation coefficients were not simply a result of longer time series availability.

3.3. Performance of SARTRAM depending on the depth of WT

Segmented regression was performed following the assumption of Burdun et al. (2023) that below a site-specific threshold represented by the calculated breakpoint, the model's ability to explain WTD diminishes.

As expected, in most cases, breaking points were different for all SARTRAM value extraction models. The depth of the breaking points for all loggers is provided in Appendix 5. The average values of breaking points for the BP model were −20.6 and −21.5 cm for VH and VV polarization, respectively. For BP500m and BP100m VH and VV models, average breaking point positions were identified at −23.0 and −22.0 cm as well as −20.0 and −19.8 cm depth, respectively. Also, breaking point values were different for SARTAM VH and VV polarizations and varied greatly among sites. The deepest WT of the breaking point for BP models was identified for the RMO5 logger at −93.6 cm in Red Moss of Balerno peatland with VH and at −73.2 cm with VV polarization for the MOI2 logger in Moine Mhor 01 peatland, Scotland. For BP500m VH and VV models, the deepest breaking point values were found for the S3 and S2 loggers (−119.8 and −82.7 cm, Sachara peatland) (Appendix 5). All the deepest breaking point values were found at sites with low average WTD. The site-average WTD at Sachara was −33.1 cm, at Red Moss of Balerno −12.2 cm, and Moine Mhor 01, −34.5 cm.

Segmented regression analysis confirmed that, despite significant variation between sites, SARTRAM values decrease with increasing water table depth. However, the rate of decline diminishes beyond the identified threshold. Furthermore, low SARTRAM and WTD *R* values are frequently observed in relation to conditions of periodic near-surface WT. These trends are well reflected in the FLANW104 (Flanders Moss peatland, Scotland) and GRE1 (Greenhead Moss peatland, Scotland) sites shown in Figure 10.

3.4. Comparison of SARTRAM performance with SAR backscatter (γ^o) signal for peatland WTD prediction

The correlation between WTD and γ^o (in both linear and dB units) across all 98 sites in 29 peatlands showed

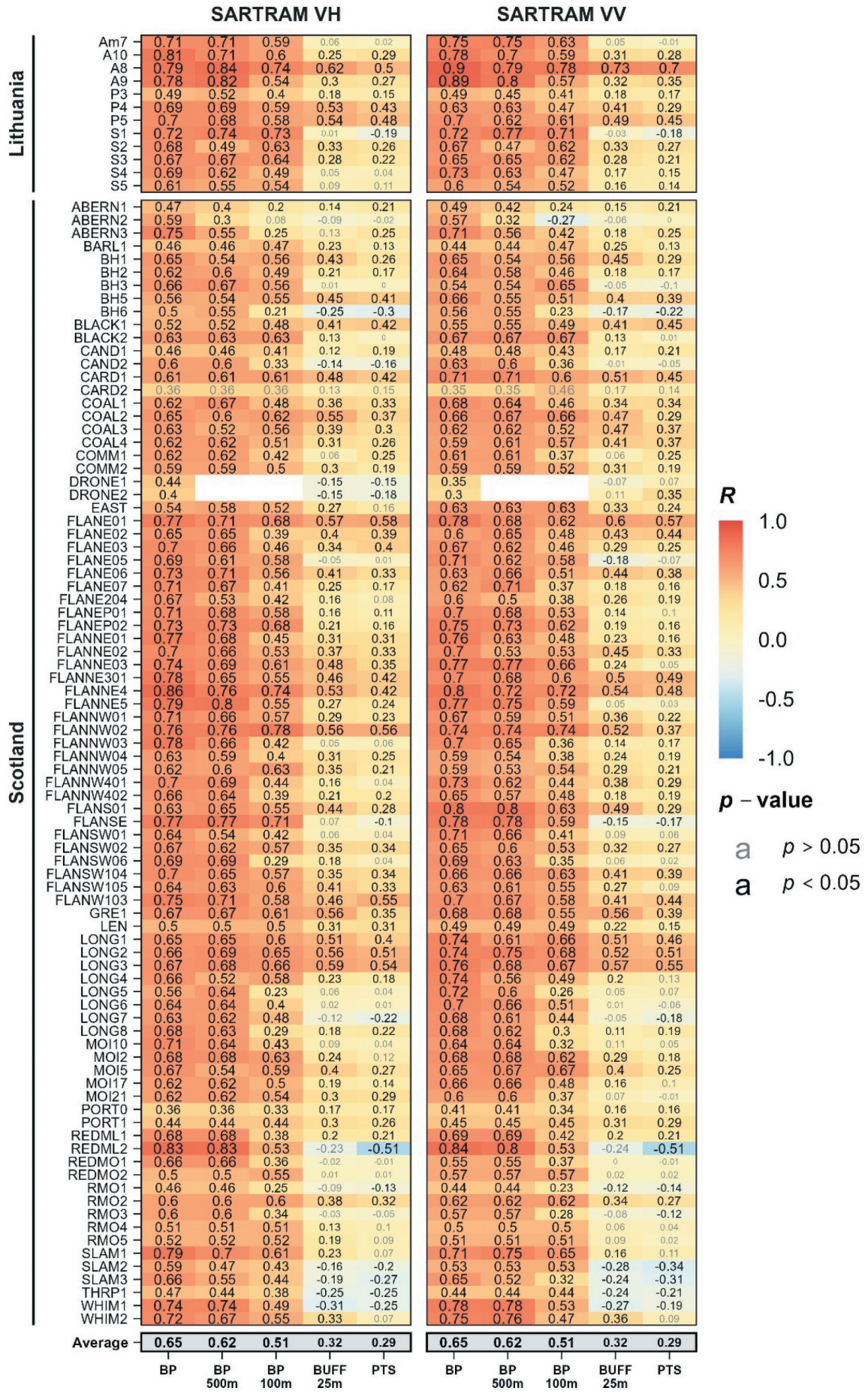

Figure 8. Spearman correlation between SARTRAM (VH and VV polarizations) with applied temporal data filtering (using moving average window) and WTD for PTS, BUFF25m, BP100m, BP500m, and BP models. Correlation values are given for all 98 loggers in 29 peatlands.

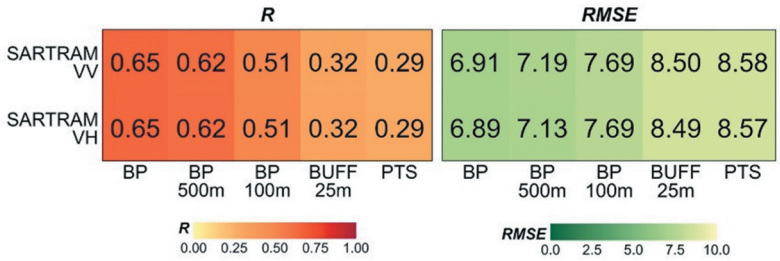

Figure 9. The average *R* and RMSE values for all SARTRAM-based WTD prediction models with applied temporal data filtering.

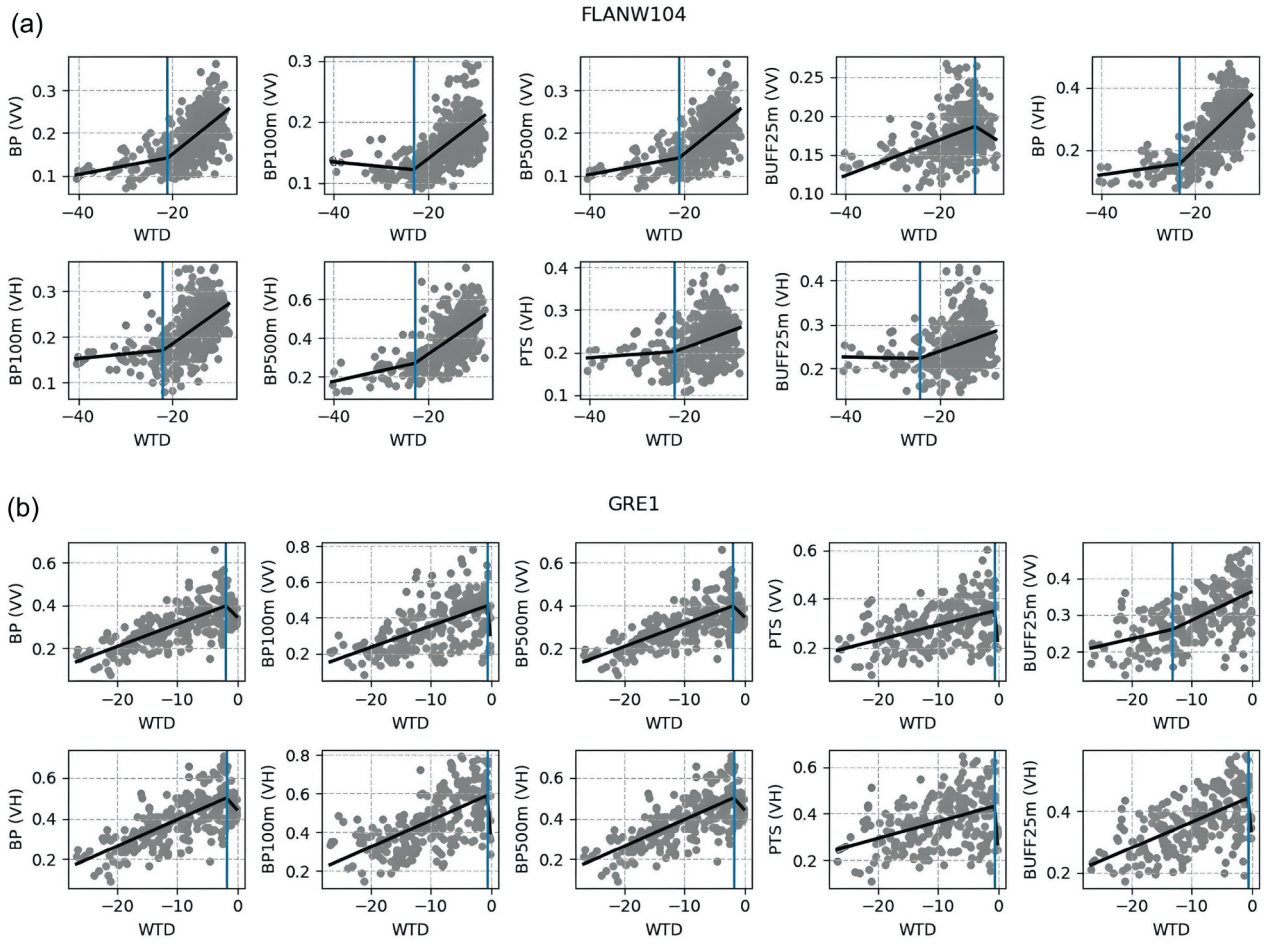

Figure 10. The scatterplots between WT and SARTRAM VH and VV with breaking points (marked with a blue line), and fitted linear regression (black line). Example of FLANW104 (a) and GRE1 (b) sites.

Table 1. Spearman correlation coefficient values between γ^o backscatter signal (in linear and dB units) in VV and VH polarizations, SARTRAM, and WTD calculated for PTS, BUFF25m, BP100m, BP500m, and BP models.

Data source	Polarization	PTS	BUFF25m	BP100m	BP500m	BP
γ^o dB	VH	0.24	0.27	0.38	0.51	0.56
	VV	0.24	0.28	0.41	0.52	0.57
γ^o linear	VH	0.24	0.27	0.38	0.51	0.56
	VV	0.24	0.28	0.41	0.52	0.57
SARTRAM	VH	0.26	0.29	0.43	0.55	0.59
	VV	0.25	0.29	0.43	0.55	0.58
γ^o db with applied MAW	VH	0.28	0.30	0.47	0.59	0.63
	VV	0.28	0.30	0.49	0.60	0.64
γ^o linear with applied MAW	VH	0.28	0.30	0.47	0.59	0.62
	VV	0.28	0.30	0.49	0.60	0.64
SARTRAM with applied MAW	VH	0.29	0.32	0.51	0.62	0.65
	VV	0.29	0.32	0.51	0.62	0.65

an extremely low R value when calculated conventionally, whereas in the PTS model, the R between γ^o and WTD reached 0.24 for both VH and VV polarizations, and in the BUFF25m models, it reached 0.27 for VH and 0.28 for VV. SARTRAM, on the other hand, showed slightly higher R scores using the PTS and BUFF25 models and in all other value extraction cases (Table 1). With BP100m, correlation values reached 0.43, while for γ^o they were 0.38 and 0.41, respectively. Similarly, for BP500m, SARTRAM reached R of 0.55, while with γ^o they were 0.51 (VH) and 0.52 (VV). Lastly, the BP method showed the same trend, for SARTRAM reaching 0.59 (VH) and 0.58 (VV), while for γ^o R was 0.56 and 0.57.

Higher R values across all γ^o analysis cases were observed using VV polarization data. This finding is consistent with other studies (Asmuß, Bechtold, and Tiemeyer 2019; Toca et al. 2023). For SARTRAM, the VV and VH polarization models demonstrated similar performance. The same trend persisted following the application of the MAW filter. Additionally, MAW filtering substantially increased the overall correlation of SARTRAM and WTD by 10.34%–18.61% across all value extraction methods (reaching 0.51, 0.62, and 0.65 for BP100m, BP500m, and BP models, respectively). A similar increase in R-values with MAW was observed for γ^o in both linear and dB units, with average increases ranging from 7.1% to 23.68% across all value extraction methods (reaching 0.49, 0.60, and 0.64 for BP100m, BP500m, and BP models, respectively).

The results suggest that the application of the MAW filter proportionally enhances the R-values. However, the correlation between γ^o and WTD with all value extraction methods remains lower than that observed between SARTRAM and WTD.

4. Discussion

4.1. Strengths and drawbacks of SARTRAM compared to OPTRAM

We introduced the synthetic aperture radar trapezoid model, the first attempt to adapt the well-recognized OPTRAM concept to the Sentinel-1 SAR data for WTD prediction in peatlands. We compared the Sentinel-1-based SARTRAM capabilities to Sentinel-2-based OPTRAM using the WTD data from 98 loggers from 29 peatlands in Scotland and Lithuania, as well as five OPTRAM and SARTRAM value extraction methods (PTS, BUFF25m, BP100m, BP500m, and BP). Based on the results of this study, OPTRAM and SARTRAM models were compared in terms of data size and continuity, computation, capabilities, and relationship with WTD.

Computation. While OPTRAM is computed using moisture and vegetation chlorophyll information derived from STR and NDVI, SARTRAM utilizes the same information derived from either VV or VH polarization backscatter for moisture and RVI index for chlorophyll. Both variables are calculated using mid-to-high spatial resolution data from the Sentinel-2 VIS-NIR and SWIR spectral ranges (10- and 20-m resolution) for OPTRAM and VV and VH polarization products Sentinel-1 GRD data (10-m spatial resolution) for SARTRAM. Consequently, both OPTRAM and SARTRAM are well-suited and have the potential for small and large spatial extent peatland investigations.

Data size and continuity. Due to optical satellite data being sensitive to cloud cover and natural light conditions, OPTRAM is limited in providing data with consistent temporal resolution, resulting in a limited number of observations with irregular frequency despite frequent Sentinel-2 revisit times. In contrast, the SAR-based SARTRAM operates independently of light and weather conditions. SAR's capability to penetrate clouds, smoke, and haze, as well as the ability to acquire data both day and night, enables the extraction of SARTRAM data with consistent high-frequency temporal resolution and offers a huge advantage compared to optical satellite data. Within the scope of this study, OPTRAM had only 10.2% of SARTRAM's observation count. The total observation count for OPTRAM was 3301, compared to 30,546 for SARTRAM. Therefore, in terms of data frequency and consistency, SARTRAM may be better suited for continuous peatland WTD monitoring compared to OPTRAM.

Capabilities in WTD prediction. Consistent with previous studies (Burdun, Bechtold, Sagris, Komisarenko, et al. 2020; Burdun, Bechtold, Sagris, Lohila, et al. 2020; Burdun et al. 2023), our results demonstrate that OPTRAM exhibits strong correlations with WTD in Lithuanian and Scottish peatlands, with an average R-value of 0.85 for BP models. All SARTRAM-based models show weaker correlations with WTD, with averages ranging from 0.25 for PTS to 0.59 for BP models without MAW and from 0.28 to 0.65 for MAW-applied PTS and BP models.

We assume that the stronger correlation rates between WTD and OPTRAM compared to WTD and SARTRAM may be determined by a number of complex reasons: (i) First, due to conceptual differences in the nature of data. The SAR backscatter signal is dependent on the dielectric constant and the targeted surface roughness. The C-band SAR signal has some (albeit limited) capability to penetrate through vegetation (El Hajj et al. 2019; Toca et al. 2022), and the backscattered microwave radiation is sensitive to the soil dielectric permittivity (Asmuß, Bechtold, and Tiemeyer 2018; Schmugge et al. 1974). In theory, this should provide reliable results for monitoring soil moisture content and WTD, including in a peatland environment. Nevertheless, in most cases, the targeted surface area "illuminated" by SAR consists of various

types and properties of individual scatterers (e.g. wind-moving plant leaves), whose backscatter signal effects on pixel information cause distortion and noise, complicating further analysis and interpretation, as well as possible results. Nevertheless, due to water absorption bands, the presence of moisture in objects can be detected through changes in spectral reflectance in SWIR bands. At the VNIR range, the chlorophyll absorption band area is also located. This provides the premise for the evaluation of plant chlorophyll content, which, among other factors, is related to water content in plants and, consequently, its content in soil. The combination of the mentioned optical data features in different ways (e.g. spectral indices, separate band analysis, trapezoid model calculation) allows to reach comparably good results. (ii) Second, the heterogeneity of surface physical conditions plays a significant role. As correctly stated by Toca et al. (2023) due to the SAR signal's complex nature, it can be affected by huge variety of physical surface properties like topography and microtopography (e.g. gullies, hags, hummocks, hollows, pools, ridges and furrow pattern), varying species composition of vegetation cover, soil density, and texture, soil, and vegetation moisture content, inundation.

Relationship with WTD. Both SARTRAM and OPTRAM values demonstrate a comparable relationship with water table depth. Consistent with findings from this and previous studies, OPTRAM values generally decrease as the water table drops (Burdun et al. 2023). However, this decline becomes less pronounced at certain depths, and at intermediate to very deep WT levels, OPTRAM values exhibit smaller variations. Similarly, SARTRAM values decrease with deeper water table levels, but this decline diminishes beyond a certain depth. This general trend is reflected in the statistical relationship between SARTRAM/OPTRAM and WTD. As WTD increases, RMSE values for SARTRAM and OPTRAM rise, while the correlation coefficient R decreases.

Low SARTRAM and WTD R values are also observed under near-surface water table conditions. This is attributed to the γ^o double-bounce scattering effect in shallowly inundated vegetation. Similar relationships have been reported in other SAR studies (Asmuß, Bechtold, and Tiemeyer 2018, 2019; Bechtold et al. 2018; Toca et al. 2023). The influence of inundation and shallow WT conditions on WTD prediction results has also been noted in OPTRAM studies using optical data (Burdun, Bechtold, Sagris, Lohila, et al. 2020).

4.2. Advantages of SARTRAM compared to the SAR backscatter signal (γ^o)

Most studies exploring the relationship between WTD and microwave backscatter have reported moderate correlation coefficients ranging from 0.38 to 0.54, depending on the study sites and the dataset used (Asmuß, Bechtold, and Tiemeyer 2018, 2019; Bechtold et al. 2018). In our study, γ^o exhibited significantly lower correlations with WTD when calculated using conventional methods (0.24 for PTS and up to 0.28 for BUFF25m). Although the R values for γ^o and WTD increased with the BP models and the application of the MAW filter, SARTRAM consistently outperformed γ^o in all the analyzed cases. The largest difference in performance between SARTRAM and γ^o was observed in the BP100m and BP500m models, with SARTRAM reaching R values of 0.62 and 0.61, respectively. Despite its overall superior performance, SARTRAM also addresses vegetation phenology and vegetation composition-specific relationship problems. Some studies suggest that seasonal and interannual variations in the correlation between γ^o and WTD are influenced not only by WTD dynamics but also by changes in biomass and vegetation phenology (Asmuß, Bechtold, and Tiemeyer 2018). In the case of the SARTRAM, as with other trapezoid models, the effect of vegetation structure and phenology is minimized by projecting two-dimensional space, where the moisture-sensitive signal is combined with a vegetation index and the model value is determined by the point location within the space. The findings of this study indicate that SARTRAM exhibits stable performance rates and low variability across different WTD dynamics conditions.

4.3. Best pixel approach and the problem of peatland area and best pixel distance to the WT measuring point

The best pixel approach, first introduced by Burdun, Bechtold, Sagris, Komisarenko, et al. (2020), significantly improves correlations between WT and the indices used. It operates under the assumption that high horizontal peat conductivity leads to the synchronization of WT and its temporal changes over a large area of peatlands. Consequently, WT dynamics detected in the best pixel can be extrapolated to a larger peatland area (Burdun, Bechtold, Sagris, Lohila, et al. 2020). We believe this assumption holds for peatlands with homogeneous surface characteristics, including surface roughness, topography, vegetation cover, and hydrological conditions. Typically, these conditions are found in undisturbed natural peatland areas rather than in cultivated peatlands or those undergoing the restoration process. However, our research indicates that the best pixel approach, without search distance limitations, is rather risky to use. This is evident when Spearman correlation coefficients (R) are calculated between WTD measurements from loggers within the same peatland (Appendix 2),

showing a negative relationship between the distance separating loggers and the correlation strength. When loggers are placed more than 1 km apart, the correlation weakens, with *R* values often falling below 0.6. This concern was also highlighted by Isoaho et al. (2024), who found that the best-pixel method can be problematic as the best pixels may not be located near WT measurement points, potentially leading to misrepresentative temporal trends, especially in restored peatlands where hydrological changes occur non-uniformly. In our case, we determined two issues related to the best-pixel approach: (i) the best-fitting SARTRAM/OPTRAM pixel, determined using the WTD values of a specific WTD logger, usually was located closer to another WTD logger within the same peatland with different WT dynamics; (ii) the best-pixel correlation coefficient value increased with the increase in peatland surface area, leading to the best pixel dependency on the peatland size. Although the correlations decrease, the issue is mitigated with the introduction of a best-pixel search buffer distance.

Figure 11 presents cases that examine whether a logger's best pixel is closest to the logger for which it was identified as the best pixel or to a different logger with different WTD values. Our research indicated that when a 500 m best pixel search buffer is applied, the match ratio within the search distance is equalized. With a 100 m buffer, the observed best pixel was generally closest to the logger for which it was determined to be the best.

The implementation of a best pixel search buffer also mitigated the impact of peatland area size on correlation values. Figure 12 illustrates the correlation between the best pixel and the size of the peatland area. Within our study sites, the OPTRAM and SARTRAM BP models demonstrated moderate correlation values between peatland surface area and the best-pixel correlation when the best pixel selection encompassed the entire peatland area. This indicates

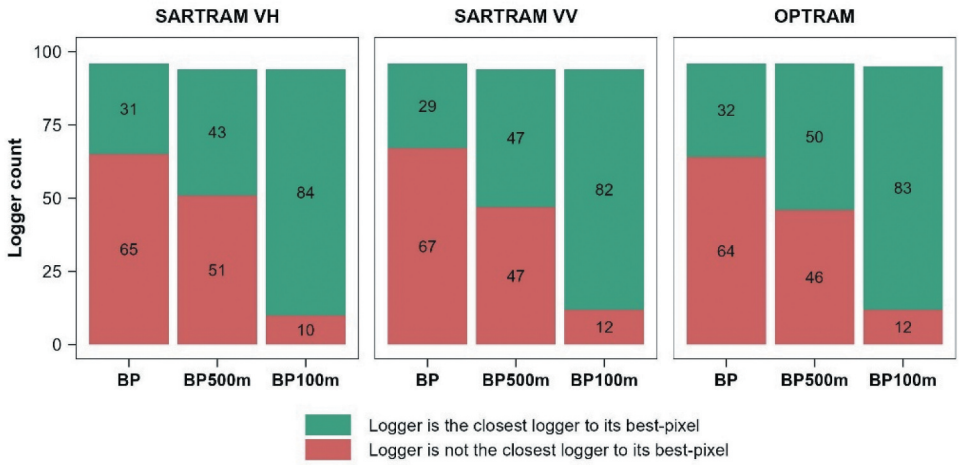

Figure 11. The number of cases WTD logger was the closest logger to its best pixel for all best-pixel-based models with SARTRAM VV, VH, and OPTRAM.

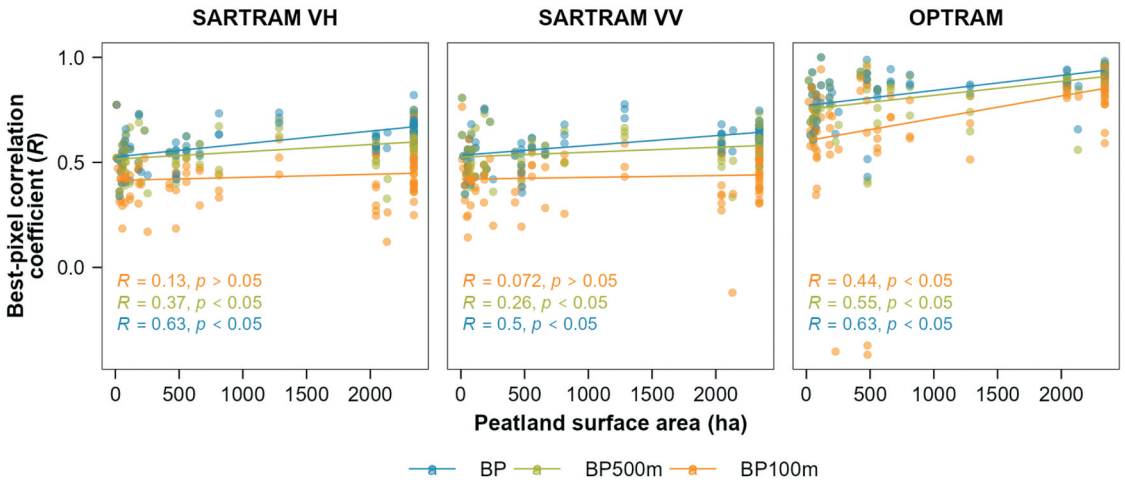

Figure 12. The relationship between the SARTRAM/OPTRAM correlation coefficient and peatland surface area for all best-pixel-based models.

that larger peatland areas are associated with higher potential *R* values. However, employing the best pixel search buffer approach resulted in reduced *R* values between the peatland surface area and the best-pixel correlation. Therefore, a clear trend is evident: as the diameter of the search buffer for the best pixel decreases, the best-pixel's correlation dependency on the peatland area also decreases.

4.4. Further possible application scenarios and optimization steps of SARTRAM

This study aimed to adapt the trapezoid model concept for use with SAR data and assess its performance, resulting in moderate to strong correlations with WTD, though generally lower than those observed between OPTRAM and WTD. However, several potential avenues for further optimization of SARTRAM are observed, which could improve its correlation with WTD in future research.

First, different corrections can be applied to SAR backscatter data before calculating SARTRAM. Several studies (Asmuß, Bechtold, and Tiemeyer 2019; Bechtold et al. 2018; Lees et al. 2021) employed angle corrections that were not applied in this study. Lees et al. (2021) suggested that these corrections could enhance results by 8.6%, whilst Bechtold et al. (2018) found that they did not significantly improve reliability. Lees et al. (2021) also identified that seasonal corrections, which account for vegetation growth, further improve results, indicating that this or other vegetation corrections possibly could improve SARTRAM performance. Together with angle and seasonal corrections and water level data smoothing, the aforementioned study achieved a mean correlation of 0.77 with VV polarization backscatter and water levels in UK wetlands.

Some studies (e.g. D'Acunha, Lee, and Johnson 2018; Jaenicke, Englhart, and Siegert 2011) have argued that in peatlands, there is a lag between changes in water table depth and subsequent changes in vegetation and surface soil properties (e.g. moisture). Jaenicke, Englhart, and Siegert (2011) reported that WTD and VH backscatter correlations increased by 0.28 with a nine-week lag. Therefore, calculating cross-correlation with a lag between water table measurements and SAR backscatter could also potentially enhance SARTRAM results.

Toca et al. (2023) also leveraged additional weather filtering and smoothing and found the best results using Random Forest Regression ($R^2 = 0.66$, RMSE = 2.1). However, it is worth noting that their model relied heavily on categorical variables, such as season and site characteristics, while SAR metrics showed lower importance. For SARTRAM, only MAW filtering was applied; however, the implementation of additional measures in future research has the potential to further enhance SARTRAM's performance.

The partial automation of determining dry and wet edges in OPTRAM, which usually requires visual interpretation (Babaeian et al. 2018; Sadeghi et al. 2017), has been achieved by Burdun et al. (2023) using Google Earth Engine (GEE). This automation could be adapted to SARTRAM in future applications.

Furthermore, SARTRAM changes the NDVI used in OPTRAM with the RVI index; however, other radar vegetation indices can also be adapted. For example, RNDVI (Mastro et al. 2023) and DSPVI (Periasamy 2018) – both applicable to Sentinel-1 GRD data – are linked to vegetation structure and biomass and could serve as alternatives. Additionally, variables derived from Sentinel-1 SLC data, such as coherence, which correlates with canopy cover (Villarroya-Carpio, Lopez-Sanchez, and Engdahl 2022), could be integrated. Some studies have also synthesized NDVI from SAR using neural networks (Calota, Faur, and Datcu 2022; Mazza et al. 2018), offering another potential substitute for NDVI. Similarly, future research could explore the feasibility of synthesizing OPTRAM from SAR data or combining OPTRAM and SARTRAM in a way that allows SARTRAM to substitute OPTRAM during cloudy conditions. Moreover, instead of using VV or VH backscatter values, indices that mitigate the influence of vegetation and enhance soil moisture estimation—such as DpRVIc (Bhogapurapu et al. 2022)—could be incorporated into SARTRAM.

The concept of SARTRAM is based on OPTRAM, which was initially used as a proxy for soil moisture (Sadeghi et al. 2017) and was first applied to peatland water table depth determination by Burdun, Bechtold, Sagris, Komisarenko, et al. (2020). SARTRAM could be utilized not only in water table depth studies but also in soil moisture research, as microwave backscatter depends on both surface roughness and soil moisture. Additionally, SARTRAM has only been employed in rewetted peatlands, which typically show lower correlation values compared to natural peatlands (Räsänen, Tolvanen, and Kareksela 2022). Therefore, applying SARTRAM to natural undisturbed peatlands with different management regimes could represent a promising direction for future research. Furthermore, we only tested SARTRAM for raised bog type peatlands. Future research should enhance the applicability of SARTRAM by evaluating its effectiveness across diverse peatland types.

Lastly, as one of the SAR advantages in predicting peatland WTD, some studies emphasize the microwave vegetation penetration capabilities (El Hajj et al. 2019; Toca et al. 2022). However, as this capability is limited to C-band, applying L-band SAR

would potentially increase penetration, leading to possibly better results by eliminating vegetation cover, biomass, and deep WT levels effect.

5. Conclusions

To overcome the limitations of OPTRAM, this paper suggested a SAR-data-based adaptation of the trapezoid model, SARTRAM, for remote peatland WTD depth monitoring. Our assessment of the SARTRAM capabilities and their comparison to OPTRAM led to the following findings:

(1) OPTRAM outperformed SARTRAM using all value extraction methods (PTS, BUFF25m, BP100m, BP500m, and BP). However, SARTRAM demonstrated considerable potential, especially when temporal filtering (moving average window) was applied, which improved correlation with WTD up to 10%–19%, and average *R* values increased to 0.65 and 0.62 for BP and BP500m models with VH polarization.
(2) SARTRAM demonstrated slightly better performance compared to traditional WTD prediction techniques based on the SAR backscatter signal.
(3) The best pixel method significantly enhances the accuracy of WTD predictions. However, two issues with the best-pixel method were observed: (i) the selected pixels were frequently positioned closer to other WTD loggers rather than the loggers from whose observations they were derived, and these neighboring loggers exhibited distinct WTD dynamics; (ii) the best-pixel correlation had a moderate-to-strong positive correlation with peatland surface area. The implementation of a best-pixel search distance buffer, although resulting in a slight reduction in WTD-SARTRAM correlation, effectively addressed these issues.
(4) The relationship between SARTRAM and WTD weakens in two specific instances: first, as WTD increases, and second, under shallow near-surface WTD conditions.

The primary advantage of SARTRAM lies in its ability to provide continuous data. Unlike OPTRAM and other optical data-based methods, SARTRAM is unaffected by cloud cover or weather conditions, ensuring temporally consistent data for predicting WTD dynamics. However, SAR data is sensitive to variations in microtopography and surface roughness, presenting an opportunity for future improvements to SARTRAM through the implementation of additional correction and filtering techniques.

Acknowledgments

We want to express our gratitude to the Foundation for Peatland Restoration and Conservation and Scotland Nature Agency for providing peatland WT in-situ data.

Author contributions

CRediT: **Laurynas Jukna:** Conceptualization, Data curation, Formal analysis, Investigation, Methodology, Resources, Supervision, Writing – original draft, Writing – review & editing; **Elzė Buslavičiūtė:** Conceptualization, Data curation, Formal analysis, Investigation, Methodology, Validation, Visualization, Writing – original draft, Writing – review & editing; **Rasa Janušaitė:** Data curation, Formal analysis, Methodology, Validation, Visualization, Writing – original draft; **Tomas Raila:** Data curation, Formal analysis, Software; **Leonas Jarašius:** Data curation, Investigation, Resources, Validation.

Disclosure statement

No potential conflict of interest was reported by the author(s).

Funding

This research was funded by the Vilnius University Science Promotion Fund in the scope of the project "Determination of water level fluctuations in restored wetlands using satellite data and machine learning methods"[Grant number MSF JM 10/2023].

Notes on contributors

Laurynas Jukna received his BSc, MSc, and PhD degrees in Geography from Vilnius University. He is currently an Assistant Professor at the Institute of Geosciences, Faculty of Chemistry and Geosciences, Vilnius University. His research interests include remote sensing and physical geography.

Rasa Janušaitė received her BSc and MSc degrees in Geography from Vilnius University, graduating Magna Cum Laude, and her PhD in Physical Geography from the State Scientific Research Institute Nature Research Centre in collaboration with Vilnius University and Klaipėda University. She is currently a Postdoctoral Fellow at the Faculty of Chemistry and Geosciences, Vilnius University, as well as a researcher at the State Scientific Research Institute Nature Research Centre. Her research interests include physical geography and the application of optical satellite remote sensing as well as GIS methods in environmental studies.

Elzė Buslavičiūt received her BSc and MSc degrees in Geography from Vilnius University, graduating Magna Cum Laude. She has also completed Erasmus+ studies in GIS and Remote Sensing at Lund University. She is currently pursuing her PhD at Vilnius University. Her research interests include remote sensing, SAR, and optical satellite data analysis, and physical geography.

Tomas Raila received his MSc and PhD degrees in Informatics from Vilnius University. He is currently a researcher at the Faculty of Mathematics and

Informatics, Vilnius University. His research interests include computational modelling, data analysis, and applied informatics.

Leonas Jarašius received his PhD degree in ecological restoration of raised peatlands from the Nature Research Centre. He is currently a nature conservation expert and ecosystem restoration specialist at the Foundation for Peatland Restoration and Conservation, Lithuania. His research interests include peatland hydrology, plant community dynamics, ecological restoration of peatlands.

ORCID

Laurynas Jukna http://orcid.org/0000-0002-3499-9989
Elzė Buslavičiūtė http://orcid.org/0009-0003-8802-2553
Rasa Janušaitė http://orcid.org/0000-0002-2025-779X
Tomas Raila http://orcid.org/0000-0001-8126-3459

Data availability statement

Sentinel-1 data accessed through Google Earth Engine (GEE) is available at https://developers.google.com/earth-engine/datasets/catalog/COPERNICUS_S1_GRD. Initial code of estimation of OPTRAM dry and wet edges available at https://github.com/PEATSPEC/EGU22_WTD_workshop. The in-situ WT datasets for Lithuania peatlands are available from the Foundation for Peatland Restoration and Conservation upon request. The in-situ WT datasets for Scotland peatlands are available at https://scotland.shinyapps.io/snh-peatland-action-hydrology-explorer/.

Declaration of generative AI and AI-assisted technologies in the writing process

During the preparation of this work, the authors used ChatGPT to improve the readability and language of the manuscript. After using this tool, the authors reviewed and edited the content as needed and take full responsibility for the content of the published article.

References

Abdelmajeed, A. Y. A., and R. Juszczak. 2024. "Challenges and Limitations of Remote Sensing Applications in Northern Peatlands: Present and Future Prospects." *Remote Sensing* 16 (3): 591. https://doi.org/10.3390/rs16030591.

Acreman, M., and J. Holden. 2013. "How Wetlands Affect Floods." *Wetlands* 33:773–786. https://doi.org/10.1007/s13157-013-0473-2.

Ahmad, S., H. Liu, A. Günther, J. Couwenberg, and B. Lennartz. 2020. "Long-Term Rewetting of Degraded Peatlands Restores Hydrological Buffer Function." *Science of the Total Environment* 749:141571. https://doi.org/10.1016/j.scitotenv.2020.141571.

Asmuß, T., M. Bechtold, and B. Tiemeyer. 2018. "Towards Monitoring Groundwater Table Depth in Peatlands from Sentinel-1 Radar Data." IGARSS 2018 - 2018 IEEE International Geoscience and Remote Sensing Symposium, Valencia, Spain: 7793–7796. IEEE. https://doi.org/10.1109/IGARSS.2018.8518838.

Asmuß, T., M. Bechtold, and B. Tiemeyer. 2019. "On the Potential of Sentinel-1 for High Resolution Monitoring of Water Table Dynamics in Grasslands on Organic Soils." *Remote Sensing* 11 (14): 1659. https://doi.org/10.3390/rs11141659.

Babaeian, E., M. Sadeghi, T. E. Franz, S. Jones, and M. Tuller. 2018. "Mapping Soil Moisture with the Optical Trapezoid Model (OPTRAM) Based on Long-Term MODIS Observations." *Remote Sensing of Environment* 211:425–440. https://doi.org/10.1016/j.rse.2018.04.029.

Bechtold, M., G. J. M. De Lannoy, R. H. Reichle, D. Roose, N. Balliston, I. Burdun, K. Devito, J. Kurbatova, M. Strack, and E. A. Zarov. 2020. "Improved Groundwater Table and L-Band Brightness Temperature Estimates for Northern Hemisphere Peatlands Using New Model Physics and SMOS Observations in a Global Data Assimilation Framework." *Remote Sensing of Environment* 246:111805. https://doi.org/10.1016/j.rse.2020.111805.

Bechtold, M., S. Schlaffer, B. Tiemeyer, and G. De Lannoy. 2018. "Inferring Water Table Depth Dynamics from ENVISAT-ASAR C-Band Backscatter Over a Range of Peatlands from Deeply-Drained to Natural Conditions." *Remote Sensing* 10 (4): 536. https://doi.org/10.3390/rs10040536.

Belyea, L. R., and N. Malmer. 2008. "Carbon Sequestration in Peatland: Patterns and Mechanisms of Response to Climate Change." *Global Change Biology* 10 (7): 1043–1052. https://doi.org/10.1111/j.1529-8817.2003.00783.x.

Beyer, F., F. Jansen, G. Jurasinski, M. Koch, B. Schröder, and F. Koebsch. 2021. "Drought Years in Peatland Rewetting: Rapid Vegetation Succession Can Maintain the Net CO_2 Sink Function." *Biogeosciences* 18:917–935. https://doi.org/10.5194/bg-18-917-2021.

Bhogapurapu, N., S. Dey, D. Mandal, A. Bhattacharya, L. Karthikeyan, H. McNairn, and Y. S. Rao. 2022. "Soil Moisture Retrieval Over Croplands Using Dual-Pol L-Band GRD SAR Data." *Remote Sensing of Environment* 271:112900. https://doi.org/10.1016/j.rse.2022.112900.

Burdun, I., M. Bechtold, M. Aurela, G. De Lannoy, A. R. Desai, E. Humphreys, S. Kareksela, et al. 2023. "Hidden Becomes Clear: Optical Remote Sensing of Vegetation Reveals Water Table Dynamics in Northern Peatlands." *Remote Sensing of Environment* 296:113736. https://doi.org/10.1016/j.rse.2023.113736.

Burdun, I., M. Bechtold, and V. Komisarenko. 2022. "Deriving Soil Moisture Information with Optical Remote Sensing Data in R, GitHub repository". Accessed February 12, 2024. https://github.com/PEATSPEC/EGU22_WTD_workshop.

Burdun, I., M. Bechtold, V. Sagris, V. Komisarenko, G. De Lannoy, and Ü. Mander. 2020. "A Comparison of Three Trapezoid Models Using Optical and Thermal Satellite Imagery for Water Table Depth Monitoring in Estonian Bogs." *Remote Sensing* 12 (12): 1980. https://doi.org/10.3390/rs12121980.

Burdun, I., M. Bechtold, V. Sagris, A. Lohila, E. Humphreys, A. R. Desai, M. B. Nilsson, G. De Lannoy, and Ü. Mander. 2020. "Satellite Determination of Peatland Water Table Temporal Dynamics by Localizing Representative Pixels of a SWIR-Based Moisture Index." *Remote Sensing* 12:2936. https://doi.org/10.3390/RS12182936.

Calota, I., D. Faur, and M. Datcu. 2022. "Estimating NDVI from SAR Images Using DNN." In *IGARSS 2022 - 2022 IEEE International Geoscience and Remote Sensing*

Symposium, 5232–5235. Kuala Lumpur, Malaysia: IEEE. https://doi.org/10.1109/IGARSS46834.2022.9884313.

Chen, Z., L. White, S. Banks, A. Behnamian, B. Montpetit, J. Pasher, J. Duffe, and D. Bernard. 2020. "Characterizing Marsh Wetlands in the Great Lakes Basin with C-Band InSAR Observations." *Remote Sensing of Environment* 242:111750. https://doi.org/10.1016/j.rse.2020.111750.

Dabrowska-Zielinska, K., M. Budzynska, M. Tomaszewska, A. Malinska, M. Gatkowska, M. Bartold, and I. Malek. 2016. "Assessment of Carbon Flux and Soil Moisture in Wetlands Applying Sentinel-1 Data." *Remote Sensing* 8 (9): 756. https://doi.org/10.3390/rs8090756.

D'Acunha, B., S. C. Lee, and M. S. Johnson. 2018. "Ecohydrological Responses to Rewetting of a Highly Impacted Raised Bog Ecosystem." *Ecohydrology* 11 (1): e1922. https://doi.org/10.1002/eco.1922.

Del Frate, F., G. Schiavon, D. Solimini, M. Borgeaud, D. H. Hoekman, and M. A. M. Vissers. 2003. "Crop Classification Using Multiconfiguration C-Band SAR Data." *IEEE Transactions on Geoscience & Remote Sensing* 41 (7): 1611–1619. https://doi.org/10.1109/TGRS.2003.813530.

Drösler, M., A. Freibauer, T. R. Christensen, and T. Friborg. 2008. "Observations and Status of Peatland Greenhouse Gas Emissions in Europe." In *The Continental-Scale Greenhouse Gas Balance of Europe*, edited by A. J. Dolman, R. Valentini, and A. Freibauer, 243–261. New York: Springer. https://doi.org/10.1007/978-0-387-76570-9_12.

El Hajj, M., N. Baghdadi, H. Bazzi, and M. Zribi. 2019. "Penetration Analysis of SAR Signals in the C and L Bands for Wheat, Maize, and Grasslands." *Remote Sensing* 11 (1): 31. https://doi.org/10.3390/rs11010031.

Esch, S. 2018. "Determination of Soil Moisture and Vegetation Parameters from Spaceborne C-Band SAR on Agricultural Areas." PhD diss., University of Cologne. http://kups.ub.uni-koeln.de/id/eprint/8047.

Fluet-Chouinard, E., B. D. Stocker, Z. Zhang, A. Malhotra, J. R. Melton, B. Poulter, J. O. Kaplan, et al. 2023. "Extensive Global Wetland Loss over the Past Three Centuries." *Nature* 614 (7947): 281–286. https://doi.org/10.1038/s41586-022-05572-6.

Gao, J., J. Holden, and M. Kirkby. 2016. "The Impact of Land-Cover Change on Flood Peaks in Peatland Basins." *Water Resources Research* 52:3477–3492. https://doi.org/10.1002/2015WR017667.

Gatis, N., P. Benaud, K. Anderson, J. Ashe, E. Grand-Clement, D. J. Luscombe, A. Puttock, and R. E. Brazier. 2023. "Peatland Restoration Increases Water Storage and Attenuates Downstream Stormflow but Does Not Guarantee an Immediate Reversal of Long-Term Ecohydrological Degradation." *Scientific Reports* 13:15865. https://doi.org/10.1038/s41598-023-40285-4.

Gong, J., N. Roulet, S. Frolking, H. Peltola, A. M. Laine, N. Kokkonen, and E. S. Tuittila. 2020. "Modelling the Habitat Preference of Two Key Sphagnum Species in a Poor Fen as Controlled by Capitulum Water Content." *Biogeosciences* 17 (22): 5693–5719. https://doi.org/10.5194/bg-17-5693-2020.

Gorelick, N., M. Hancher, M. Dixon, S. Ilyushchenko, D. Thau, and R. Moore. 2017. "Google Earth Engine: Planetary-Scale Geospatial Analysis for Everyone." *Remote Sensing of Environment* 202:18–27. https://doi.org/10.1016/j.rse.2017.06.031.

Gorham, E. 1991. "Northern Peatlands: Role in the Carbon Cycle and Probable Responses to Climatic Warming." *Ecological Applications* 1 (2): 182–195. https://doi.org/10.2307/1941811.

Harris, A., and R. G. Bryant. 2009. "A Multi-Scale Remote Sensing Approach for Monitoring Northern Peatland Hydrology: Present Possibilities and Future Challenges." *Journal of Environmental Management* 90 (7): 2178–2188. https://doi.org/10.1016/j.jenvman.2007.06.025.

Harris, A., R. G. Bryant, and A. J. Baird. 2006. "Mapping the Effects of Water Stress on Sphagnum: Preliminary Observations Using Airborne Remote Sensing." *Remote Sensing of Environment* 100 (3): 363–378. https://doi.org/10.1016/j.rse.2005.10.024.

Holden, J., Z. E. Wallage, S. N. Lane, and A. T. McDonald. 2011. "Water Table Dynamics in Undisturbed, Drained and Restored Blanket Peat." *Journal of Hydrology* 402 (1–2): 103–114. https://doi.org/10.1016/j.jhydrol.2011.03.010.

Holtgrave, A. K., N. Röder, A. Ackermann, S. Erasmi, and B. Kleinschmit. 2020. "Comparing Sentinel-1 and -2 Data and Indices for Agricultural Land Use Monitoring." *Remote Sensing* 12 (18): 2919. https://doi.org/10.3390/RS12182919.

Höper, H., J. Augustin, J. P. Cagampan, M. Drösler, L. Lundin, E. J. Moors, H. Vasander, J. M. Waddington, and D. Wilson. 2008. "Restoration of Peatlands and Greenhouse Gas Balances." In *Peatlands and Climate Change*, edited by M. Strack, 182–210. Jyväskylä: International Peat Society.

Hrysiewicz, A., E. P. Holohan, S. Donohue, and H. Cushnan. 2023. "SAR and InSAR Data Linked to Soil Moisture Changes on a Temperate Raised Peatland Subjected to a Wildfire." *Remote Sensing of Environment* 291:113516. https://doi.org/10.1016/j.rse.2023.113516.

Hyyryläinen, A., M. Turunen, P. Rautio, and S. Huttunen. 2018. "Sphagnum Mosses in a Changing UV-B Environment: A Review." *Perspectives in Plant Ecology, Evolution and Systematics* 33:1–8. https://doi.org/10.1016/j.ppees.2018.04.001.

Isoaho, A., L. Ikkala, L. Päkkilä, H. Marttila, S. Kareksela, and A. Räsänen. 2024. "Multi-Sensor Satellite Imagery Reveals Spatiotemporal Changes in Peatland Water Table After Restoration." *Remote Sensing of Environment* 306:114144. https://doi.org/10.1016/j.rse.2024.114144.

Jaenicke, J., S. Englhart, and F. Siegert. 2011. "Monitoring the Effect of Restoration Measures in Indonesian Peatlands by Radar Satellite Imagery." *Journal of Environmental Management* 92 (3): 630–638. https://doi.org/10.1016/j.jenvman.2010.09.029.

Kartiwa, B. S. H., H. Adi, N. Sosiawan, P. Heryani, A. Rejekiningrum, I. Dariah Maswar Lenin, and W. Widiyono. 2023. "Water Level and Soil Moisture Monitoring for Peatland Fire Risk Indicator." *IOP Conference Series: Earth and Environmental Science* 1201 (1): 012066. https://doi.org/10.1088/1755-1315/1201/1/012066.

Kasischke, E., L. Bourgeau-Chavez, A. Rober, H. W. Kevin, J. M. Waddington, and M. R. Turetsky. 2008. "Effects of Soil Moisture and Water Depth on ERS SAR Backscatter Measurements from an Alaskan Wetland Complex." *Remote Sensing of Environment* 113 (9): 1868–1873. https://doi.org/10.1016/j.rse.2009.04.006.

Kasischke, E. S., and L. L. Bourgeau-Chavez. 1997. "Monitoring South Florida Wetlands Using ERS-1 SAR Imagery." *Photogrammetric Engineering & Remote Sensing* 63 (3): 281–291.

Kim, J. W. 2013. Applications of Synthetic Aperture Radar (SAR)/SAR Interferometry (InSAR) for Monitoring of Wetland Water Level and Land Subsidence. Report 503. Ohio: Ohio State University.

Kim, J. W., Z. Lu, L. Gutenberg, and Z. Zhu. 2017. "Characterizing Hydrologic Changes of the Great Dismal Swamp Using SAR/InSAR." *Remote Sensing of Environment* 198:187–202. https://doi.org/10.1016/j.rse.2017.06.009.

Kim, Y., and J. J. Van Zyl. 2009. "A Time-Series Approach to Estimate Soil Moisture Using Polarimetric Radar Data." *IEEE Transactions on Geoscience & Remote Sensing* 47:2519–2527. https://doi.org/10.1109/TGRS.2009.2014944.

Klinke, R., H. Kuechly, A. Frick, M. Förster, T. Schmidt, A. K. Holtgrave, B. Kleinschmit, D. Spengler, and C. Neumann. 2018. "Indicator-Based Soil Moisture Monitoring of Wetlands by Utilizing Sentinel and Landsat Remote Sensing Data." *PFG – Journal of Photogrammetry, Remote Sensing and Geoinformation Science* 86:71–84. https://doi.org/10.1007/s41064-018-0044-5.

Köchy, M., R. Hiederer, and A. Freibauer. 2015. "Global Distribution of Soil Organic Carbon – Part 1: Masses and Frequency Distributions of SOC Stocks for the Tropics, Permafrost Regions, Wetlands, and the World." *Soil* 1:351–365. https://doi.org/10.5194/soil-1-351-2015.

Krzepek, K., J. Schmidt, and D. Iwaszczuk. 2022. "Fusion of SAR and Multi-Spectral Time Series for Determination of Water Table Depth and Lake Area in Peatlands." *PFG – Journal of Photogrammetry, Remote Sensing and Geoinformation Science* 90:561–575. https://doi.org/10.1007/s41064-022-00216-w.

Kumar, D., S. Rao, and J. R. Sharma. 2013. "Radar Vegetation Index as an Alternative to NDVI for Monitoring of Soyabean and Cotton." *Indian Cartographer* 33:91–96.

Kwon, M. J., A. Ballantyne, P. Ciais, C. Qiu, E. Salmon, N. Raoult, B. Guenet, et al. 2022. "Lowering Water Table Reduces Carbon Sink Strength and Carbon Stocks in Northern Peatlands." *Global Change Biology* 28 (22): 6752–6770. https://doi.org/10.1111/gcb.16394.

Lees, K. J., R. R. E. Artz, D. Chandler, T. Aspinall, C. A. Boulton, J. Buxton, N. R. Cowie, and T. M. Lenton. 2021. "Using Remote Sensing to Assess Peatland Resilience by Estimating Soil Surface Moisture and Drought Recovery." *Science of the Total Environment* 761:143312. https://doi.org/10.1016/j.scitotenv.2020.143312.

Le Hégarat-Mascle, S., M. Zribi, F. Alem, A. Weisse, and C. Loumagne. 2002. "Soil Moisture Estimation from ERS/SAR Data: Toward an Operational Methodology." *IEEE Transactions on Geoscience & Remote Sensing* 40:2647–2658. https://doi.org/10.1109/TGRS.2002.806994.

Leifeld, J., and L. Menichetti. 2018. "The Underappreciated Potential of Peatlands in Global Climate Change Mitigation Strategies." *Nature Communications* 9:1071. https://doi.org/10.1038/s41467-018-03406-6.

Linkevičienė, R., R. Šimanauskienė, G. Kibirkštis, O. Grigaitė, and J. Taminskas. 2023. "Hydrological and Botanical Diversity of a Raised Bog and Its Evaluation Using In Situ and Remote Sensing Methods." *Journal of Hydrology* 617:129119. https://doi.org/10.1016/j.jhydrol.2023.129119.

Littlewood, N., P. Anderson, R. Artz, O. Bragg, P. Lunt, and R. Marrs. 2010. "Peatland Biodiversity." The IUCN UK Peatland Programme. https://researchportal.plymouth.ac.uk/en/publications/peatland-biodiversity-report-to-iucn-uk-peatland-programme/.

Loisel, J., and A. Gallego-Sala. 2022. "Ecological Resilience of Restored Peatlands to Climate Change." *Communications Earth & Environment* 3:208. https://doi.org/10.1038/s43247-022-00547-x.

Loisel, J., A. V. Gallego-Sala, M. J. Amesbury, G. Magnan, G. Anshari, D. W. Beilman, J. C. Benavides, et al. 2021. "Expert Assessment of Future Vulnerability of the Global Peatland Carbon Sink." *Nature Climate Change* 11 (1): 70–77. https://doi.org/10.1038/s41558-020-00944-0.

Main-Knorn, M., B. Pflug, J. Louis, V. Debaecker, U. Müller-Wilm, and F. Gascon. 2017. "Sen2Cor for Sentinel-2." *Proceedings of SPIE - Image and Signal Processing for Remote Sensing* 23: 10457. https://doi.org/10.1117/12.2278218.

Martin-Ortega, J., T. E. H. Allott, K. Glenk, and M. Schaafsma. 2014. "Valuing Water Quality Improvements from Peatland Restoration: Evidence and Challenges." *Ecosystem Services* 9:34–43. https://doi.org/10.1016/j.ecoser.2014.06.007.

Mastro, P., M. D. Peppo, A. Crema, M. Boschetti, and A. Pepe. 2023. "Statistical Characterization and Exploitation of Synthetic Aperture Radar Vegetation Indexes for the Generation of Leaf Area Index Time Series." *International Journal of Applied Earth Observation and Geoinformation* 124:103498. https://doi.org/10.1016/j.jag.2023.103498.

Mazza, A., M. Gargiulo, R. Gaetano, and G. Scarpa. 2018. "Estimating the NDVI from SAR by Convolutional Neural Networks." In *IGARSS 2018 - 2018 IEEE International Geoscience and Remote Sensing Symposium*, 1954–1957. Valencia, Spain: IEEE. https://doi.org/10.1109/IGARSS.2018.8519459.

McNeil, P., and J. M. Waddington. 2003. "Moisture Controls on Sphagnum Growth and CO2 Exchange on a Cutover Bog." *Journal of Applied Ecology* 40:354–367. https://doi.org/10.1046/j.1365-2664.2003.00790.x.

Meingast, K. M., M. J. Falkowski, E. S. Kane, L. R. Potvin, B. W. Benscoter, A. M. S. Smith, L. L. Bourgeau-Chavez, and M. E. Miller. 2014. "Spectral Detection of Near-Surface Moisture Content and Water-Table Position in Northern Peatland Ecosystems." *Remote Sensing of Environment* 152:536–546. https://doi.org/10.1016/j.rse.2014.07.014.

Millard, K., and M. Richardson. 2018. "Quantifying the Relative Contributions of Vegetation and Soil Moisture Conditions to Polarimetric C-Band SAR Response in a Temperate Peatland." *Remote Sensing of Environment* 206:123–138. https://doi.org/10.1016/j.rse.2017.12.011.

Millard, K., D. K. Thompson, M. A. Parisien, and M. Richardson. 2018. "Soil Moisture Monitoring in a Temperate Peatland Using Multi-Sensor Remote Sensing and Linear Mixed Effects." *Remote Sensing* 10:903. https://doi.org/10.3390/rs10060903.

Mohammadimanesh, F., B. Salehi, M. Mahdianpari, B. Brisco, and M. Motagh. 2018a. "Wetland Water Level Monitoring Using Interferometric Synthetic Aperture Radar (InSAR): A Review." *Canadian Journal of Remote Sensing* 44:247–262. https://doi.org/10.1080/07038992.2018.1477680.

Mohammadimanesh, F., B. Salehi, M. Mahdianpari, B. Brisco, and M. Motagh. 2018b. "Multi-Temporal, Multi-Frequency, and Multi-Polarization Coherence and SAR Backscatter Analysis of Wetlands." *ISPRS Journal of Photogrammetry & Remote Sensing*

142:78–93. https://doi.org/10.1016/j.isprsjprs.2018.05.009.
Mohan, R. R., B. Paul, S. Mridula, and P. Mohanan. 2015. "Measurement of Soil Moisture Content at Microwave Frequencies." *Procedia Computer Science* 46:1238–1245. https://doi.org/10.1016/j.procs.2015.01.040.
Mullissa, A., A. Vollrath, C. Odongo-Braun, B. Slagter, J. Balling, Y. Gou, N. Gorelick, and J. Reiche. 2021. "Sentinel-1 SAR Backscatter Analysis Ready Data Preparation in Google Earth Engine." *Remote Sensing* 13:1954. https://doi.org/10.3390/rs13101954.
Nasirzadehdizaji, R., F. B. Sanli, S. Abdikan, Z. Cakir, A. Sekertekin, and M. Ustuner. 2019. "Sensitivity Analysis of Multi-Temporal Sentinel-1 SAR Parameters to Crop Height and Canopy Coverage." *Applied Sciences* 9:655. https://doi.org/10.3390/app9040655.
Nijp, J. J., K. Metselaar, J. Limpens, H. M. Bartholomeus, M. B. Nilsson, F. Berendse, and S. E. A. T. M. van der Zee. 2019. "High-Resolution Peat Volume Change in a Northern Peatland: Spatial Variability, Main Drivers, and Impact on Ecohydrology." *Ecohydrology* 12 (6): e2114. https://doi.org/10.1002/eco.2114.
Nugent, K. A., I. B. Strachan, M. Strack, N. T. Roulet, and L. Rochefort. 2018. "Multi-Year Net Ecosystem Carbon Balance of a Restored Peatland Reveals a Return to Carbon Sink." *Global Change Biology* 24:5751–5768. https://doi.org/10.1111/gcb.14449.
Page, S. E., and A. J. Baird. 2016. "Peatlands and Global Change: Response and Resilience." *Annual Review of Environment and Resources* 41 (1): 35–57. https://doi.org/10.1146/annurev-environ-110615-085520.
Pakalne, M., J. Etzold, M. Ilomets, L. Jarašius, P. Pawlaczyk, K. Bociag, I. Chlost, et al. 2021. *Best Practice Book for Peatland Restoration and Climate Change Mitigation - Experiences from LIFE Peat Restore Project*. Riga: University of Latvia.
Parry, L. E., J. Holden, and P. J. Chapman. 2014. "Restoration of Blanket Peatlands." *Journal of Environmental Management* 133:193–205. https://doi.org/10.1016/j.jenvman.2013.11.033.
Peatland Action. 2024. "Hydrological Monitoring Data Explorer" [dataset]. Accessed February 26, 2024. https://scotland.shinyapps.io/snh-peatland-action-hydrology-explorer/.
Periasamy, S. 2018. "Significance of Dual Polarimetric Synthetic Aperture Radar in Biomass Retrieval: An Attempt on Sentinel-1." *Remote Sensing of Environment* 217:537–549. https://doi.org/10.1016/j.rse.2018.09.003.
Pschenyckyj, C., T. Donahue, M. Kelly-Quinn, C. O'Driscoll, and F. Renou-Wilson. 2023. "An Examination of the Influence of Drained Peatlands on Regional Stream Water Chemistry." *Hydrobiologia* 850:3313–3339. https://doi.org/10.1007/s10750-023-05188-5.
Quesney, A., S. Le Hégarat-Mascle, O. Taconet, D. Vidal-Madjar, J. P. Wigneron, C. Loumagne, and M. Normand. 2000. "Estimation of Watershed Soil Moisture Index from ERS/SAR Data." *Remote Sensing of Environment* 72 (3): 290–303. https://doi.org/10.1016/S0034-4257(99)00102-9.
Ranghetti, L., M. Boschetti, F. Nutini, and L. Busetto. 2020. "'Sen2r': An R Toolbox for Automatically Downloading and Preprocessing Sentinel-2 Satellite Data." *Computers and Geosciences* 139:104473. https://doi.org/10.1016/j.cageo.2020.104473.
Räsänen, A., A. Tolvanen, and S. Kareksela. 2022. "Monitoring Peatland Water Table Depth with Optical and Radar Satellite Imagery." *International Journal of Applied Earth Observation and Geoinformation* 112:102866. https://doi.org/10.1016/j.jag.2022.102866.
Reddin, E., J. Hanafin, M. Tong, L. Gill, and M. G. Healy. 2025. "Modelling Water Table Depth at Rewetted Peatlands with Sentinel-1 and Sentinel-2." *Science of Remote Sensing* 11:100238. https://doi.org/10.1016/j.srs.2025.100238.
Reynolds, N., B. Mota, and J. M. Nightingale. 2025. "Open-Access Satellite Data for Peatland Condition and Restoration Monitoring in the UK: A Review." *Frontiers in Environmental Science* 13:1685165. https://doi.org/10.3389/fenvs.2025.1685165.
Sadeghi, M., E. Babaeian, M. Tuller, and S. B. Jones. 2017. "The Optical Trapezoid Model: A Novel Approach to Remote Sensing of Soil Moisture Applied to Sentinel-2 and Landsat-8 Observations." *Remote Sensing of Environment* 198:52–68. https://doi.org/10.1016/j.rse.2017.05.041.
Schimelpfenig, D. W., D. J. Cooper, and R. A. Chimner. 2014. "Effectiveness of Ditch Blockage for Restoring Hydrologic and Soil Processes in Mountain Peatlands." *Restoration Ecology* 22:257–265. https://doi.org/10.1111/rec.12053.
Schmugge, T., P. Gloersen, T. Wilheit, and F. Geiger. 1974. "Remote Sensing of Soil Moisture with Microwave Radiometers." *Journal of Geophysical Research* 79:317–323. https://doi.org/10.1029/JB079i002p00317.
Schwieger, S., J. Kreyling, J. Couwenberg, M. Smiljanić, R. Weigel, M. Wilmking, and G. Blume-Werry. 2021. "Wetter Is Better: Rewetting of Minerotrophic Peatlands Increases Plant Production and Moves Them Towards Carbon Sinks in a Dry Year." *Ecosystems* 24:1093–1109. https://doi.org/10.1007/s10021-020-00570-z.
Shuttleworth, E. L., M. G. Evans, M. Pilkington, T. Spencer, J. Walker, D. Milledge, and T. E. H. Allott. 2019. "Restoration of Blanket Peat Moorland Delays Stormflow from Hillslopes and Reduces Peak Discharge." *Journal of Hydrology X* 2:100006. https://doi.org/10.1016/j.hydroa.2018.100006.
Šimanauskienė, R., R. Linkevičienė, M. Bartold, K. Dąbrowska-Zielińska, G. Slavinskienė, D. Veteikis, and J. Taminskas. 2019. "Peatland Degradation: The Relationship Between Raised Bog Hydrology and Normalized Difference Vegetation Index." *Ecohydrology* 12 (8): e2195. https://doi.org/10.1002/eco.2159.
Skriver, H. 2012. "Crop Classification by Multitemporal C- and L-Band Single- and Dual-Polarization and Fully Polarimetric SAR." *IEEE Transactions on Geoscience & Remote Sensing* 50:2138–2149. https://doi.org/10.1109/TGRS.2011.2172994.
Swindles, G. T., P. J. Morris, D. J. Mullan, R. J. Payne, T. P. Roland, M. J. Amesbury, M. Lamentowicz, et al. 2019. "Widespread Drying of European Peatlands in Recent Centuries." *Nature Geoscience* 12 (11): 922–928. https://doi.org/10.1038/s41561-019-0462-z.
Tampuu, T., J. Praks, R. Uiboupin, and A. Kull. 2020. "Long Term Interferometric Temporal Coherence and DInSAR Phase in Northern Peatlands." *Remote Sensing* 12:1566. https://doi.org/10.3390/rs12101566.
Toca, L., R. R. E. Artz, C. Smart, T. Quaife, K. Morrison, A. Gimona, R. Hughes, M. H. Hancock, and D. Klein. 2023. "Potential for Peatland Water Table Depth Monitoring Using Sentinel-1 SAR Backscatter: Case Study of Forsinard Flows, Scotland, UK." *Remote Sensing* 15 (7): 1900. https://doi.org/10.3390/rs15071900.
Toca, L., K. Morrison, R. R. E. Artz, A. Gimona, and T. Quaife. 2022. "High Resolution C-Band SAR

Backscatter Response to Peatland Water Table Depth and Soil Moisture: A Laboratory Experiment." *International Journal of Remote Sensing* 43:5231–5251. https://doi.org/10.1080/01431161.2022.2131478.

Torbick, N., A. Persson, D. Olefeldt, S. Frolking, W. Salas, S. Hagen, P. Crill, and C. Li. 2012. "High Resolution Mapping of Peatland Hydroperiod at a High-Latitude Swedish Mire." *Remote Sensing* 4:1974–1994. https://doi.org/10.3390/rs4071974.

Trudel, M., F. Charbonneau, and R. Leconte. 2012. "Using RADARSAT-2 Polarimetric and ENVISAT-ASAR Dual-Polarization Data for Estimating Soil Moisture Over Agricultural Fields." *Canadian Journal of Remote Sensing* 38:514–527. https://doi.org/10.5589/m12-043.

Tuba, Z., N. G. Slack, and L. R. Stark. 2011. "The Ecological Value of Bryophytes as Indicators of Climate Change." In *Bryophyte Ecology and Climate Change*, edited by Z. Tuba, N. G. Slack, and L. R. Stark, 3–12. Cambridge: Cambridge University Press. https://doi.org/10.1017/cbo9780511779701.002.

Udali, A., E. Lingua, and H. J. Persson. 2021. "Assessing Forest Type and Tree Species Classification Using Sentinel-1 C-Band SAR Data in Southern Sweden." *Remote Sensing* 13:3237. https://doi.org/10.3390/rs13163237.

Ulaby, F. T., R. K. Moore, and A. K. Fung. 1986. "Microwave Remote Sensing: Active and Passive." In *From Theory to Applications*. From Theory to Applications. Vol. 3. Norwood, MA: Artech House.

UNEP. 2022. "Global Peatlands Assessment – The State of the World's Peatlands: Evidence for Action Toward the Conservation, Restoration, and Sustainable Management of Peatlands." In *Main Report*, edited by D. Kopansky. Nairobi: United Nations Environment Programme. Accessed March 10, 2025. https://www.unep.org/resources/global-peatlands-assessment-2022.

Villarroya-Carpio, A., J. M. Lopez-Sanchez, and M. E. Engdahl. 2022. "Sentinel-1 Interferometric Coherence as a Vegetation Index for Agriculture." *Remote Sensing of Environment* 280:113208. https://doi.org/10.1016/j.rse.2022.113208.

Walker, R. Z., D. S. Boyd, R. Andersen, and D. J. Large. 2025. "InSAR Coherence Linked to Soil Moisture, Water Level and Precipitation on a Blanket Peatland in Scotland." *Remote Sensing* 17 (21): 3507. https://doi.org/10.3390/rs17213507.

Whittington, P., M. Strack, R. Van Haarlem, S. Kaufman, P. Stoesser, J. Maltez, J. S. Price, and M. Stone. 2007. "The Influence of Peat Volume Change and Vegetation on the Hydrology of a Kettle-Hole Wetland in Southern Ontario, Canada." *Mires and Peat* 2:9. https://doi.org/10.19189/001c.128250.

Xu, L., H. Zhang, C. Wang, B. Zhang, and M. Liu. 2019. "Crop Classification Based on Temporal Information Using Sentinel-1 SAR Time-Series Data." *Remote Sensing* 11 (1): 53. https://doi.org/10.3390/rs11010053.

Yu, Z., J. Loisel, D. P. Brosseau, D. W. Beilman, and S. J. Hunt. 2010. "Global Peatland Dynamics Since the Last Glacial Maximum." *Geophysical Research Letters* 37: L13402. https://doi.org/10.1029/2010GL043584.

Zribi, M., N. Baghdadi, N. Holah, and O. Fafin. 2005. "New Methodology for Soil Surface Moisture Estimation and Its Application to ENVISAT-ASAR Multi-Incidence Data Inversion." *Remote Sensing of Environment* 96:485–496. https://doi.org/10.1016/j.rse.2005.04.005.